Proposal and Practical Research for “Module Drug Discovery” Regarding Anticancer Drugs

抗がん剤におけるモジュール創薬の提唱と実践的研究

2018

Kenzo Iizuka

飯 塚 健 蔵

Proposal and Practical Research for “Module Drug Discovery” Regarding Anticancer Drugs

2018

Kenzo Iizuka

Contents

List of Abbreviations

5-FU	5-fluorouracil
AML	acute myeloid leukemia
ANOVA	analysis of variance
Cytarabine	cytosine arabinoside, ara-C, cytarabine
AUC	area under the curve, pharmacokinetics
BLI	bioluminescence imaging
BWC	changes in body weight
CDDP	cisplatin
CDHP	5-chloro-2, 4-dihydroxypyridine
CI	continuous infusion
C_{max}	maximum concentration, pharmacokinetics
CNDAC	2'-C-Cyano-2'-deoxy-1-β-D-arabino-pentofranocylcytosine, DFP-10917
CNDACTP	CNDAC 5'-triphosphate
Ct	Threshold Cycle
CTA	citrazinic acid
CYP	cytochrome P450, liver microsomes
ddCNC	2'-Ccyano-2',3 '-didehydro-2',3 '-dideoxycytidine
DNA	deoxyribonucleic acid
DNA pol	DNA polymerase
DOPC	dioleoylphosphatidylcholine
DOPE	dioleoyl-phosphatidylethanolamine
DPD	dihydropyrimidine dehydrogenase
EA	ethyl acetate
EGFR	epidermal growth factor receptor
EM-FU	1-ethoxymethyl-5-fluorouracil
FOLFIRI	5-fluorouracil, leucovorin and irinotecan
FOLFOX	5-fluorouracil, leucovorin and oxaliplatin
FUMP	5-fluorouridine-5'-monophosphate
GEM	gemcitabine
GI	gastrointestinal
HCl	hydrochloric acid
HER-2	human epidermal growth factor receptor 2
HFS	hand-foot syndrome
HLPC	high-performance liquid chromatography

IC_{50}, IC_{70}	50% inhibitory concentration, 70% inhibitory concentration
ILS	increase in lifespan
ip	intraperitoneal
IR	inhibition rate of tumor growth
iv	intravenously
KOH	potassium hydroxide
mRNA	messenger RNA
MST	median survival time
MTD	maximum tolerance dose
NK	natural killer
OPRT	orotate phosphoribosyltransferase
OXO	oteracil
PC	peritoneal carcinomatosis
PCR	polymerase chain reaction
PEG	polyethylene glycol
PK	pharmacokinetics
PLT	platelet
QOL	quality of life
RBC	red blood cell
RNA	ribonucleic acid
RNAi	RNA interference
rRNA	ribosomal RNA
RT	real-time
RTV	relative tumor volume
S-1	tegafur-gimeracil-oteracil
SD	standard deviation
shRNA	short-hairpin RNA
$T_{1/2}$	half-life, pharmacokinetics
TCA	trichloroacetic acid
TGI	tumor growth inhibition
T_{max}	time of maximum concentration, pharmacokinetics
TS	thymidylate synthase
TYMS	thymidylate synthase gene
UFT	tegafur-uracil
WBC	white blood cell

Animals

- BALB/cA jcl-nu nude mice
- C.B-17/Icr-scid Jcl immunodeficient mice
- F344/N-nu nude rats

Tumor cells

- AZ521 human gastric cancer cell, GC
- BxPC-3 human pancreatic cancer cell, PC
- CCRF-CEM human leukemia cell
- CoLo320DM human colorectal cancer cell, CRC
- HeLa human cervical carcinoma cell
- HT-29 human colorectal cancer cell, CRC
- KM20C human colorectal cancer cell, CRC
- Lu-99 human lung ancer cell
- MKN-45 human gastric cancer cell, GC
- MV-4-11 human acute myelocytic leukemia cell
- PAN-4 human pancreatic cancer cell, PC
- Panc-1 human pancreatic cancer cell, PC
- SKOV-3 human ovarian cancer cell
- U937 human lymphoma cell

Chapter 1 General Introduction

There are a lot of medicines for treatment of diseases. The medicines are provided in clinical practice through several strategies of drug discovery and development. The process of drug discovery and development is well known that it takes 10–17 years from target selection to market launch and it is lower than 10% for the probability of success[1]. The common process of drug discovery involves some stages, including target identification and validation, lead identification by using high-throughput screening, medicinal chemistry and lead optimization, and drug candidate selection. Other methods of drug discovery and development have been applied in accordance with the period which is shorter than a conventional method and the success rate which requires higher than a common method. These different ways of the drug discovery are founded on all one-on-one relationships with a disease effector site and a substance. Although new drugs are invented by the conventional strategies, it is not necessarily sufficient for patient benefit especially in the anticancer drugs[2]. Because it is inferred that many researchers and physicians focus only on cancer and do not focus on cancer patients. Most of cancer patients do not really want side effects and insufficient curative effects, and this is issues confronting the cancer chemotherapy. In order to solve the problem in such side effects and unsatisfied curative effects, it is necessary to start drug discovery from the beginning, and then the existing drugs have also been screened and survived by the long history of evidence based medicine. However, this one-on-one methodology takes a long time to provide the new improved drugs to the cancer patients, and it is not easy in response to demands from the cancer patients. Therefore, as one of the solution, the author proposes a new strategy of drug discovery, "Module Drug Discovery", which is assemble components by a convertible functional unit, “Module”. Examples of “Module” include

small molecular, polymer, antibody and nucleic acid, but are not limited to, administration method, dose, route, targeted disease, prodrug and drug delivery systems. This is the strategy to improve and modify the active substances in module units based on the efficacy and safety information for cancer patients, and to create a new substance.

In this dissertation, the three examples of anticancer drugs are presented as a practical research by using the module drug discovery. In the first example, it is described that new promising antimetabolite, DFP-11207, was discovered as the upgrading the active substance focused on an oral fluorouracil by the exchanging and assembling three modules based on the toxicity and safety information of existing drug for cancer patients. In the second example, it is described that novel deoxycytidine analog, DFP-10917, was practical researched as the embodiment of functional mechanism and effectiveness *in vivo* by using the functional conversion for the module of administration method and targeted disease focused on unique mechanism in vitro based on the information of existing drugs and cancer patients. In the third example, it is described that DFP-10825 was developed as the assembling deliver and administration system focused on a RNA interference of active substance in the basic research based on the information of peritoneal disseminated cancer patients.

These examples support the proposal for “module drug discovery”. The chapters below are provided to discuss this significance and their specific drug-discovery and research.

Chapter 2 Proposal for "Module Drug Discovery" Regarding Anticancer Drugs

Many drugs have been discovered in universities or biotechnology companies based on many of the medical, scientific and technological factors[3]. It is well known to demonstrate a clear link between the contribution of medicines and the satisfaction of patients, and these are over 50% contribution and satisfaction for an about 70% disease[4]. Even among them, recent advance in new anticancer drugs has focused on low molecular weight tyrosine kinase inhibitors and monoclonal antibodies for various growth factor receptors to specifically that have been shown abnormal in tumors to minimize toxicities by traditional chemotherapies in various advanced and/or metastatic cancers[5]. In parallel, the surrogate biomarker discovery and development have been capable for detecting various gene amplifications and mutations such as epidermal growth factor receptor (EGFR) and human epidermal growth factor receptor 2 (HER-2), etc. in tumors and support molecular-targeted drugs development or precision medicine for tumor patients[6]. However, only one-third of patients respond to such new medicines with a high refractory matter and much higher health care burden being created. On the other hand, the traditional cytotoxic agents including platinum drugs, taxanes, and antimetabolites are still the main stream of anticancer therapy that have been used to improve a clinical response and quality of life (QOL) of cancer patients[7]. Amid the situation, many anticancer drugs including molecular-targeted drugs lack the balance between efficacy and safety to cancer patients in almost cancerous tumors.

Meanwhile, the process of drug discovery and development is well known that it takes 10–17 years from target selection to market launch and it is lower than 10% for the probability of success[1]. Each process includes multiple process units relating to one

another, and an exploratory early discovery, a lead identification, a lead optimization, preclinical studies, clinical phase 1 studies, clinical phase 2 studies, clinical phase 3 studies and a registration to regulatory agency are assigned to each process unit. One of the most important process among them is the drug discovery as the decisive factor in achieving market launch. The common process of drug discovery involves some stages, including target identification and validation, lead identification by using high-throughput screening, medicinal chemistry and lead optimization, and drug candidate selection. While this drug-discovering method is significant in the selection of drug candidate, but the drug candidate have an uncertain regarding the occurrence of side effects until clinical studies or market launch as indicated Figure 2.1.

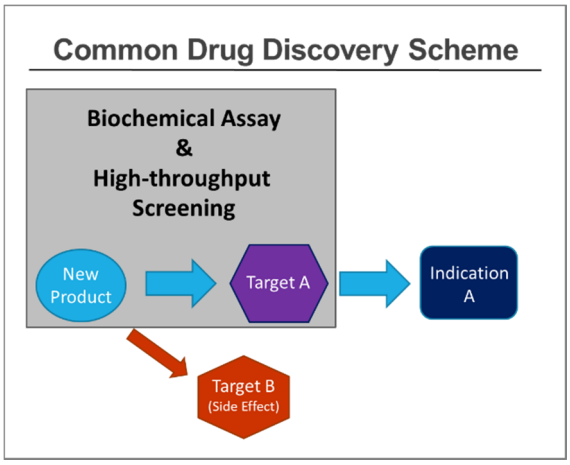

Figure 2.1. Common drug discovery scheme including the occurrence of side effects at clinical studies or market launch.

One of the solutions, the author propose a new strategy of drug discovery, “Module Drug Discovery”, which is constructed by using substances or functions as constituent units based on the information on efficacy and safety in patients. Wherein, “Module” is defined as a convertible functional unit as pharmaceutical viewpoint. In

general terms, “Module” means only “chemical compound” in a narrow sense such as “small molecular”, “polymer”, “antibody” and “nucleic acid” etc., but in a broad sense it means “all functional unit” such as “administration”, “dose”, “route”, “prodrug”, “drug delivery systems” and “disease” etc. In other words, the creators recognize each element of drugs as functional conversion for modulator by biochemical approach and assemble them to develop new pharmaceutical products as though it was introduced a strategy for general-purpose engineering approach used in manufacturing products or functional units. For example, such as automobiles have progressed from petrol motorcars to electric motorcars, and telephones have progressed from land-line phones to mobile phones, anybody knows the strategies which almost all of manufacturing products have been improved by upgrading or replacing modules.

“Modular drug discovery” is adapted the existing drug used strategy to drug discovery, in similar to approach by “Drug repositioning” as shown Figure 2.2.

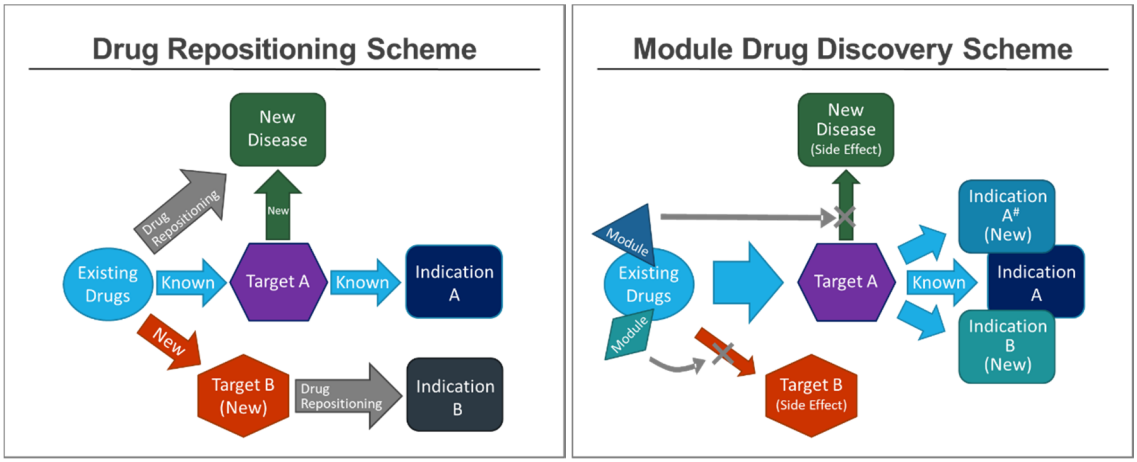

Specific example
- Thalidomide: Sleep medication ⇨ Multiple myeloma
- Raloxifene: Breast cancer drug ⇨ Osteoporosis

Specific example
- 5-FU: UFT (Tegafur + Uracil) ⇨
  S-1 (Tegafur + Gimeracil + Oteracil)

Figure 2.2 Difference between drug repositioning scheme and module drug discovery scheme.

Drug repositioning is identifying and developing new uses for existing drugs[8]. Repositioning existing drugs for new indications could deliver the productivity increases which the industry needs while shifting the locus of production, because they can offer a better risk-versus-reward trade-off as compared with other drug development strategies. On the other side, module drug discovery is modifying or adding functional components to the existing drugs. Inventions of patentable drug development by using the modules can be considered as module drug discovery.

A number of strategy models have been proposed from the viewpoint of efficient in the drug discovery and development. “High-throughput screening” and “virtual screening” are important components of drug discovery research[9]. In addition, “Chorus model” uses a small internal staff of experienced drug developers and a network of external vendors to design and implement chemistry, manufacturing and control processes, preclinical toxicology and biology, and early clinical trials[10]. On the other hand, a large-scale “cross-species molecular network association” approach for targeted drug screening from natural sources by using omics analysis strategy and modular pharmacology is presented[11]. However, these all drug discovery models are constructed from a researcher's standpoint in contrast the module drug discovery. Other methods of drug discovery and development have been applied in accordance with the period which is shorter than a conventional method and the success rate which requires higher than a common method. These different ways of the drug discovery are founded on all one-on-one relationships with a disease effector site and a substance.

As an example of common drug-discovery, a positive response in a first step of screening in a biochemical assay identifies the primary ‘hit’ compounds against the target, and goes into more screens by filter of physicochemical and pharmacological properties,

a hit becomes a 'lead' compounds, and then one new product is selected by a final step of chemical refinement and biological screening before finally entering clinical testing[1]. On the other hand, "Module drug discovery" is approached to the making and developing products from the patient angle by the three steps as described below (Figure 2.3).

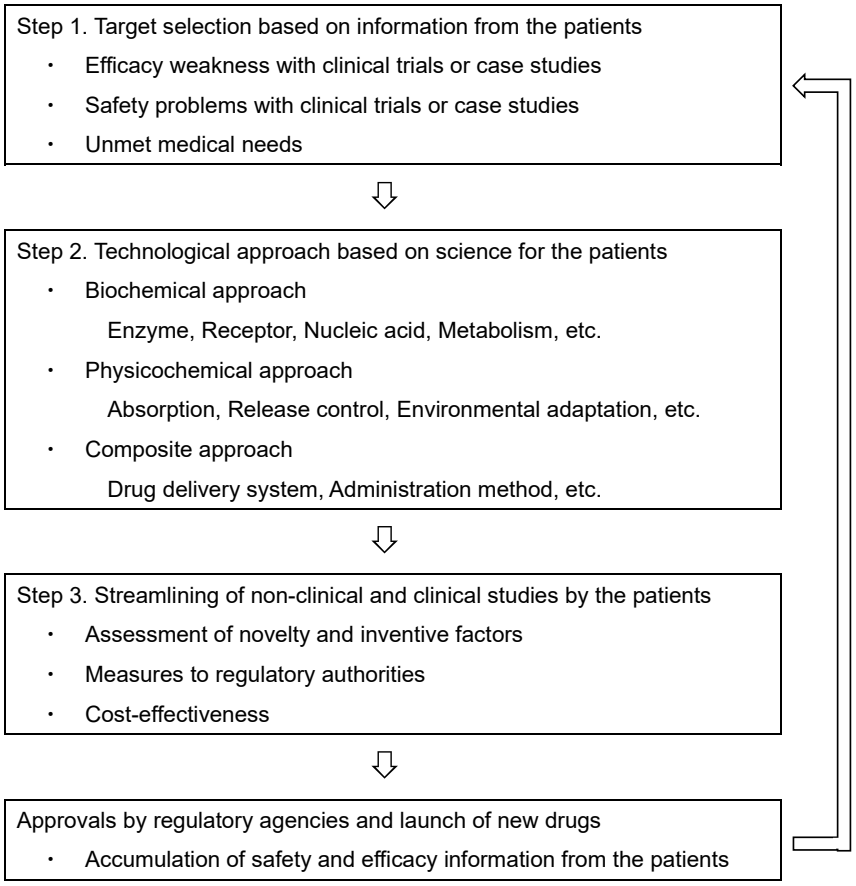

Figure 2.3. The flow of drug development by the module drug discovery.

Each step for the flow of module drug discovery perform the target selection and technological approach by the module units, and the assembling and exchanging modules take biochemical or physiochemical and composite approach for possible solution to various problems. In case of a cancer drug, the approved drug (cytotoxic agents,

molecular target agents, immuno-modulators or their active molecules) and the useful cancer target (solid tumor or hematological cancer, and elder or intractable cancer patients) are selected, and then the minimized toxicity and maximized efficacy are strived by the upgrading module units. Consequently, patentable products, low cost and high speed production can be materialized. The approach of module drug discovery by assembling and exchanging parts from patient information such as “Lego Block Type Approach” make a huge difference compared to the approach of traditional or novel drug discovery by one-on-one relationships with disease effector site and substance such as “Jigsaw Puzzle Type Approach”. Therefore, the important thing is that the module drug discovery listen to the voice of the patients, the target for which is derived from the patients, the approaches of which are exercised by the scientific technique for the patients, and the benefits of which are enjoyed by the patients.

Chapter 3 Drug Discovery of New Promising Antimetabolite, DFP-11207

3.1 Introduction

5-Fluorouracil (5-FU), one of antimetabolites, discovered and synthesized since late 1950's, introduced clinically[12], has been widely used as a single agent or in combination with other cytotoxic drugs called as 5-fluorouracil/leucovorin/oxaliplatin (FOLFOX)[13], 5-fluorouracil/leucovorin/irinotecan (FOLFIRI)[14], 5-fluorouracil/cisplatin (FP)[15], and so on for cancer patients with mainly advanced and metastatic gastrointestinal (GI) or GI cancers. Clinical response and toxicity of 5-FU have been remarkably influenced by its dosing schedule and a continuous infusion (CI) of 5-FU has been found to increase the response rates of patients with GI cancers[16-19]. Furthermore, Lokich *et al*[20] showed that a long-term CI of 5-FU resulted in a higher response with mild to severe GI toxicity and a rapid bolus injection of 5-FU showed in a lower response with severe myelosuppression in their randomized phase III study. Also, 5-FU has been shown to be rapidly hydrolyzed to its inactive form inducing cardio- and neurotoxicity and/or hand-foot-syndrome (HFS), while, a phosphorylated form of 5-FU has been indicated to cause GI- and myelo-toxicity in addition to its antitumor activity.

To adopt the advantage of a long-time CI of 5-FU and patient compliance from a viewpoint of QOL in patients, several oral 5-FU derivatives such as capecitabine (Hoffman-La Roche Ltd., Basel, Switzerland)[21], tegafur-uracil (UFT; Taiho Pharmaceutical Ltd., Tokyo, Japan)[22], and tegafur-gimeracil-oteracil (S-1; Taiho Pharmaceutical Ltd.)[23] have been developed and widely applied to the treatment of cancer patients. However, these oral fluoropyrimidines do not completely separate the efficacy from 5-FU-induced toxicities, and therefore, dose-reduction or pause of the drug

treatment are required for cancer patients. Incidentally, the primary dose-limiting toxicity of capecitabine, UFT and S-1 has been shown to be HFS[24], GI toxicity[25] and hematological toxicity[26], respectively. Therefore, it is an unmet medical need for developing a new version of oral 5-FU drug that minimizes such adverse events without compromising the antitumor activity of oral fluoropyrimidines.

Especially, S-1 is combination drug which is obtained by blending three components, tegafur, 5-chloro-2,4-dihydroxypyridine (CDHP) and potassium oxonate (Oxo). Tegafur (FT) is a prodrug of 5-FU which exhibits an excellent anticancer action, CDHP inhibits dihydropyrimidin dehydrogenase (DPD) which degrade 5-FU to inactive form, and Oxo inhibits orotate phosphoribosyltransferase (OPRT) which leads 5-FU-induced toxicity in GI tract (Figure 3.1)[27]. Regard the three components of the combination drug as each module, it can be said that S-1 is truly a product of "Module Drug Discovery". However, S-1 has an issue with impossibility of the continued therapy by myelotoxicity including thrombopenia for some patients despite the sophisticated drug. With that kind of background, it is necessary to convert the key components of module for resolve the issues of S-1 from the patient information as the strategy for "Module Drug Discovery".

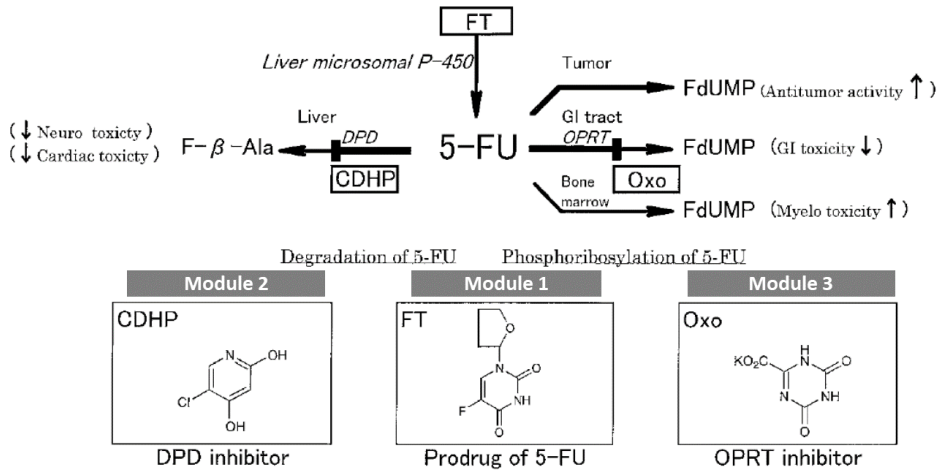

Figure 3.1. Biochemical action and chemical structure of S-1[27]

Based on the same mode of action as S-1, a new promising oral fluoropyrimidine prodrug, DFP-11207 (5-chloro-2-(3-(3-(ethoxymethyl)-5-fluoro-2,6-dioxo-1,2,3,6-tetrahydopyrimidine-1-carbonyl)benzoyloxy)pyridine-4-yl-2,6-bis (propionyloxy) isonicotinate) shown in Figure 3.2. This single molecule is intelligently designed and consists of three important components, 1-ethoxymethyl-5-fluorouracil (EM-FU), 5-chloro-2, 4-dihydroxypyridine (CDHP) and citrazinic acid (CTA) to exhibit augmented antitumor activity in various human cancers without the toxicities described above by cooperating the three distinctive functional components as each module.

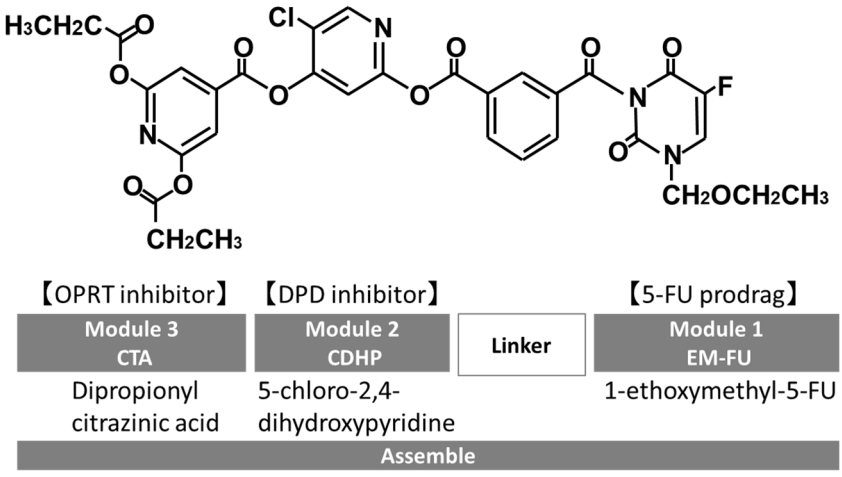

Figure 3.2. Molecular structure of DFP-11207 (MW: 713.02).

The possible metabolism and mechanism of action of DFP-11207 indicate Figure 3.3. After oral administration, DFP-11207 is quickly hydrolyzed to three major metabolites, EM-FU, CDHP, and CTA in GI cells, and resultant EM-FU is further metabolized to 5-FU by liver microsomes. CDHP inhibits the degradation of 5-FU into inactive catabolite in the liver, which results in a higher 5-FU levels in the body. CTA mainly distributes and inhibits the phosphorylation of 5-FU in GI cells leading to decrease in GI toxicity.

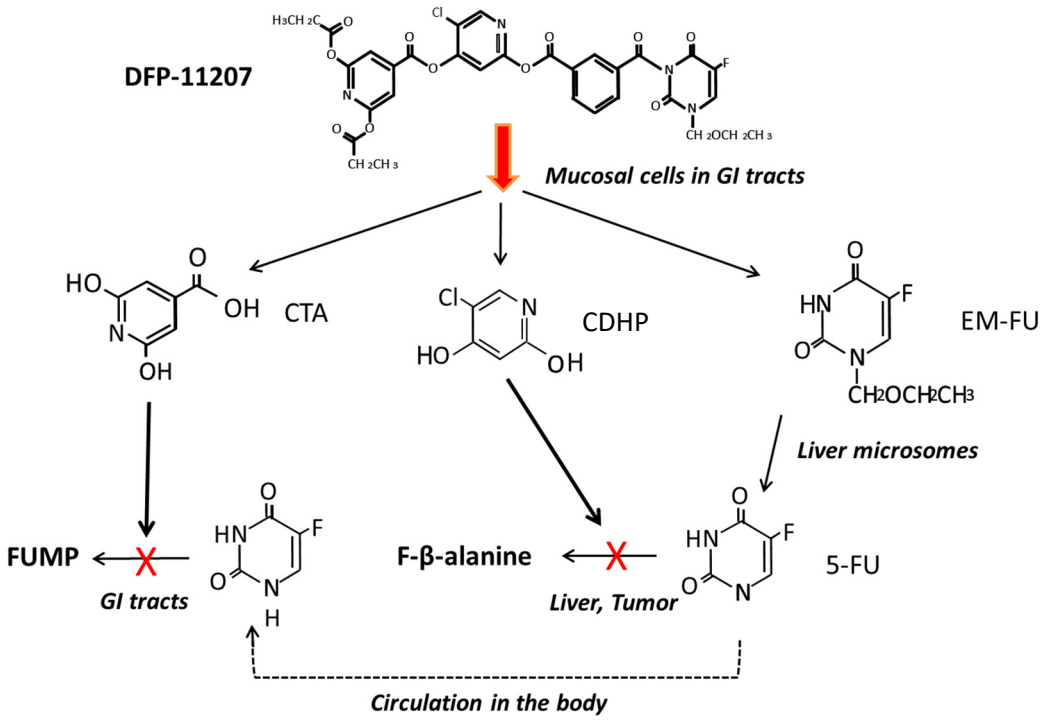

Figure 3.2. Possible biological metabolism and mechanism of action of DFP-11207.

In this research, DFP-11207 which it was made drug discovery by each module is ascertained the validity of the allegations from the pharmacokinetics and pharmacodynamics profiles and the antitumor activities *in vitro* and *in vivo*. In addition, this research is conducted to compare the difference of the S-1 and DFP-11207 based on conversion from FT to EM-FU as the 5-FU prodrug (Module 1), non-conversion of CDHP as DPD inhibitor (Module 2), and conversion from Oxo to CTA as OPRT inhibitor (Module 3), which the assembling three components focused on the toxicity and antitumor activity of S-1 as the module drug discovery.

3.2 Materials and methods

3.2.1 Materials.

5-FU and CTA were purchased from Sigma Chemical Co (St Louis, MO, USA). CDHP (gimeracil) was supplied from Tokyo Chemical Industry Co., Ltd (Tokyo, Japan). EM-FU and DFP-11207 were synthesized in Delta-Fly Pharma, Inc. (Tokushima, Japan). [6-^{3}H]-5-FU (710 GBq.mmol) was obtained from New England Nuclear Co. (Tokyo, Japan). All other chemical and biochemical materials were standard commercial products.

3.2.2 Animals and tumor cells.

F344/N-nu nude rats (5-week old) were purchased from CLEA Japan Inc. (Tokyo, Japan) and were fed with a sterilized pellet diet and autoclaved water ad libitum. Rats were kept in laminar air-flow units throughout experiments performed.

Human colorectal cancer cells (CoLo320DM, KM12C, and HT-29), pancreatic cancer cells (Panc-1 and BxPC-3) and gastric cancer cell (AZ521) were obtained from ATCC (The Global BioSource Center, Manassas, VA, USA) and maintained *in vitro* as a monolayer culture in a RPMI-1640 medium supplemented with heat-inactivated fetal calf serum containing penicillin (100 U/mL), streptomycin (100 ug/mL) and L-glutamine (2 mM) until used for *in vitro* and *in vivo* experiments.

3.2.3 Antitumor experiments.

The care and treatment of the animals were in accordance with the guidelines issued by the Science and International Affairs Bureau of the Japanese Ministry of Education, Science, Culture and Sports. The experimental protocol was performed after approval from the Institutional Animal Ethical Committee in Delta-Fly Pharma, Inc.

Groups of six nude rats were used. Human tumor xenografts were prepared by subcutaneous implantation of cultured tumor cells (1 to 5 x 10^6 cells) into the right axilla of rats. When each tumor volume reached about ~100-200 mm^3, DFP-11207 and S-1 (combination of 1 M tegafur, 0.4 M gimeracil, and 1 M oteracil) were administered orally for 14-21 consecutive days. 5-FU and gemcitabine were intraperitoneally (ip) injected daily for 5 days and weekly for 3 weeks, respectively. The tumor volume [1/2 x (the major axis) x (the minor axis)^2] was measured twice a week throughout the experiments, relative tumor volume (RTV) was calculated as follows:

RTV =

(mean tumor volume during therapy) / (mean tumor volume at the start of therapy).

The antitumor effects of drugs tested were estimated by the following equation:

mean inhibition rate of tumor growth (IR, %) =

(1-[mean RTV of drug-treated group / mean RTV of control group] x 100).

3.2.4 Enzyme assay.

Activity of dihydropyrimidine dehydrogenase (DPD) catalyzing 5-FU degradation and orotate phosphoribosyltransferase (OPRT) catalyzing 5-FU phosphorylation were determined according to the method of Shirasaka *et al*[26].

3.2.5 Intracellular phosphorylation of 5-FU and its subsequent incorporation into RNA in intact cells *in vitro*.

According to the method described previously[28], CoLo320DM cells (2 x 10^7) suspended in a RPMI-1640 medium were incubated with 1 uM [6-^{3}H] 5-FU (37 kBq) alone or in the presence of DFP-11207 and CTA in a final volume of 2 mL at 37℃ for

45 min and then 2 mL of 10% trichloroacetic acid (TCA) were added. The mixtures were centrifuged at 2,000 rpm for 5 min, and the TCA-soluble fraction was neutralized with KOH and 50 ul aliquots were subjected to silica gel thin layer chromatography. The spot of 5-fluorouridine-5'-monophosphate (FUMP) was scrapped off for measurement of its radioactivity. The radioactivity incorporated into RNA present in the TCA-precipitated material was extracted by the method of Schneider[29] for determination of the amount of 5-FU incorporated into RNA.

3.2.6 *In vitro* hydrolysis of DFP-11207.

DFP-11207 (1 mM) was incubated with rat serum, and 20% (w/v) homogenates extracted from rat liver and small intestine at 37℃ for 10-60 min and then 10% TCA was added to the reaction mixture followed by centrifugation at 3,000x *g* for 10 min. The resultant supernatant was neutralized with 2 M KOH solution and subjected to high-performance liquid chromatography (HPLC) to determine the contents of EM-FU, CDHP and CTA produced.

3.2.7 Extraction and determination of 5-FU and CTA in the blood and tissues.

DFP-11207 was orally administered to AZ521 tumor-bearing nude rats. The animals were sacrificed at the times indicated, and their blood and tissues were rapidly removed. The tumors and small intestines were homogenized with three volumes of ice-cold saline and centrifuged at 10,000x *g* for 30 min. The supernatant obtained were used as crude extracts containing 5-FU and CTA. The extraction and determination of 5-FU in the blood and tissues were performed according to the method reported previously[30].

3.2.8 Extraction and determination of 5-FU concentration in the blood of rats.

Rats were treated with DFP-11207 or S-1, then sacrificed at various indicated times and their blood were rapidly removed and centrifuged to obtain the serum samples. One milliliter of the serum was added to 0.1 mL of the known amount of the internal standard solution (5-bromouracil) for 5-FU and shaken with 5 mL of ethyl acetate (EA) twice. The two EA layers were combined and evaporated at 40℃ under a gentle stream of N_2 gas. The residue was dissolved in distilled water, passed through a 0.45 μm filter and the 5-FU content of the filtrate was determined by the method described previously[31].

3.2.9 Pathological evaluation of injury of the digestive tracts.

The degree of GI injury of drug-treated rats was evaluated pathologically as described in the previous paper[28]. In this experiment, rough microscopic changes in GI tract of rats treated with DFP-11207, S-1, and tegafur-gimeracil (molar ratio; 1:0.4) as negative control were observed.

3.2.10 Statistical analysis.

The significance of differences between groups and/or drugs with or without treatment was assessed using Dunnett's test and the Student's *t*-test.

3.3 Results

3.3.1 Enzymatic hydrolysis of DFP-11207 *in vitro*.

DFP-11207 consists of three important components, EM-FU, CDHP, and CTA, and needs to be cleaved by the hydrolysis to functional metabolites which then exhibit biological activities. Using rat plasma and crude homogenates from the rat liver and small

intestine, time-dependent hydrolysis of DFP-11207 was investigated as shown in Figure 3.4. Three metabolites, EM-FU, CDHP, and CTA were formed in a time dependent manner, and the majority of metabolites was produced within 60 min in this assay system. However, 5-FU was not produced from EM-FU, the prodrug of 5-FU by this enzymatic reaction. On the other hand, DFP-11207 was found to be stable and not to be hydrolyzed in phosphate-buffered saline solution alone (data not shown).

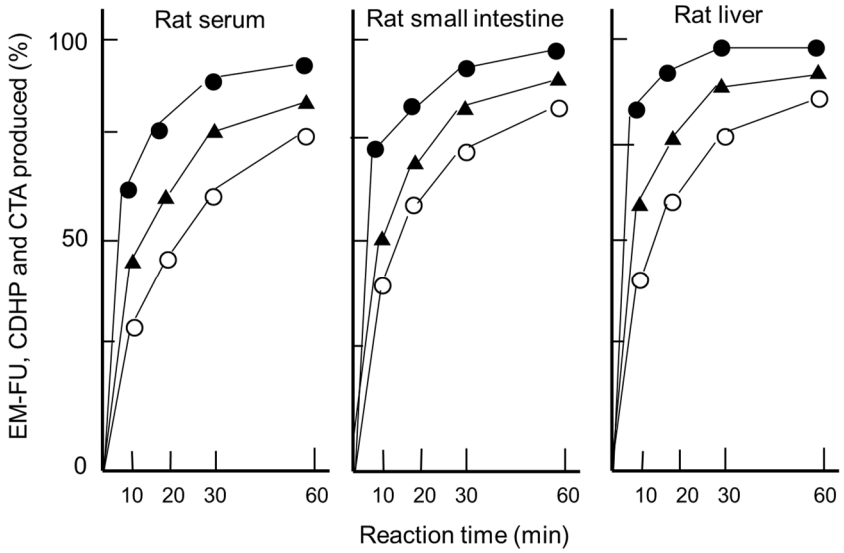

Figure 3.4. Enzymatic conversion of DFP-11207 to three metabolites, EM-FU, CDHP, and CTA in the serum, liver and small intestine of rats *in vitro*.

DFP-11207 (1 mM/assay mixture) was incubated with rat serum or with crude extracts of the liver and small intestine of rats. After 10, 20, 30 and 60 min, the reaction was terminated and the products, EM-FU (●), CDHP (○), and CTA (▲) were measured using HPLC system. Data represent mean values for duplicate assays.

3.3.2 Inhibition by DFP-11207 of DPD and OPRT activities *in vitro*.

The degree of Inhibition activity of DFP-11207 was evaluated using crude extracts of the rat liver for DPD and of SC-2 tumors for OPRT shown in Table 3.1. DFP-11207 inhibited both DPD and OPRT activities dose-dependently, indicating that DFP-11207

was promptly hydrolyzed to each component, CDHP and CTA, and exhibited their inhibitiory activities to both DPD and OPRT. However, DFP-11207 did not inhibit both DPD and OPRT activities when heat-denatured crude extracts was used in the assay, suggesting that the intact DFP-11207 has no inhibitory activity (data not shown).

Table 3.1. Inhibitory effect of DFP-11207 on the activities of DPD and OPRT

Inhibition of DPD				Inhibition of OPRT			
Drug	Conc. (μM)	Activity (nmol/ml/min)	Inhibition (%)	Drug	Conc. (μM)	Activity (nmol/ml/min)	Inhibition (%)
Control	-	0.667	-	Control	-	0.335	-
DFP-11207	20	0.131	80.4	DFP-11207	20	0.003	99.1
	2	0.152	77.2		2	0.079	76.4
	0.2	0.374	43.9		0.2	0.242	27.8
	0.02	0.518	22.3				

Crude extracts of rat liver and human tumor xenografts (SC-2) were used as enzyme souses of DPD and OPRT, respectively. Dara represent mean values for duplicate enzyme assays.

3.3.3 Effect of DFP-11207 on intracellular phosphorylation of 5-FU and its subsequent incorporation into RNA.

CTA has been reported to strongly inhibit OPRT activity (5-FU phosphorylation) in cell-free tumor extract but not intact cells *in vitro*, suggesting no transport of it into the cells[28]. When incubated with 1 μM [6-^{3}H] 5-FU, DFP-11207 inhibited dose-dependently the intracellular phosphorylation of 5-FU and its subsequent incorporation into RNA in Colo320DM cells while CTA alone did not inhibit as expected shown in Figure 3.5. This result indicates that after incorporated into the cells, DFP-11207 is rapidly cleaved, and resultant CTA freed from intact DFP-11207 could inhibit the intracellular formation of F-nucleotides from 5-FU incorporated into the cells.

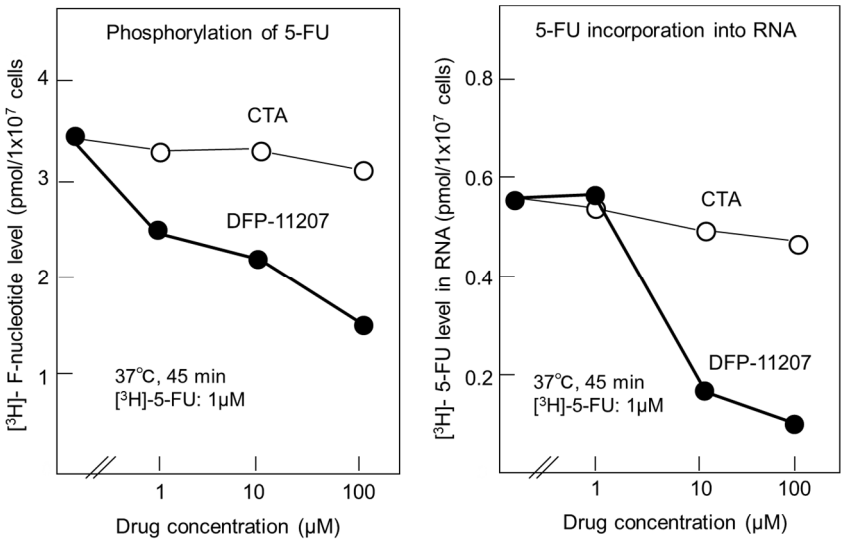

Figure 3.5. Inhibitory effects of DFP-11207 and citrazinic acid on intracellular phosphorylation of 5-FU and its subsequent incorporation into RNA in human colorectal tumor cells.

One to 100 μM DFP-11207 and CTA were added to colorectal tumor cells (1 x 10^7 cells) and incubated with 1μM 5-FU containing [6-^{3}H] 5-FU at 37℃ for 45min. After the reaction, treated cells were isolated by centrifugation at 4℃, immediately treated with 10% PCA to separate the acid-soluble fraction containing the nucleotide form of 5-FU and acid-insoluble fraction containing 5-FU-incorporated RNA. Data represent mean values for duplicate cellular assays.

3.3.4 Conversion of EM-FU, prodrug of 5-FU, to active 5-FU by various liver microsomes.

Tegafur (FT), prodrug of 5-FU is well known to be hydrolyzed to 5-FU by liver microsomes, mainly by CYP2A6 species. As EM-FU shows a similar chemical structure of FT, the conversion of EM-FU to 5-FU *in vitro* by intact liver microsomes derived from various species was investigated. As shown in Figure 3.6.A. EM-FU was hydrolyzed similarly in rat, monkey and human microsomes (~30-60 pmol/min/mg) except for dog microsomes which showed the lowest conversion rate of EM-FU to 5-FU. Next, to specify

a subgroup of CYPs catalyzing the conversion of EM-FU to 5-FU, an inhibitory activity for the activation of EM-FU was examined using chemical compounds inhibiting each CYP enzyme. As shown in Figure 3.6.B, the conversion of EM-FU to 5-FU was strongly inhibited by coumarin, α-naphthoflavone, *p*-nitrophenol, and toleandomycin, indicating that EM-FU is converted to 5-FU by CYP1A2, CYP2A6, CYP2E1, and CYP 3A4, respectively. And these data seem to be quite different from tegafur being hydrolyzed by only CYP2A6 (data not shown).

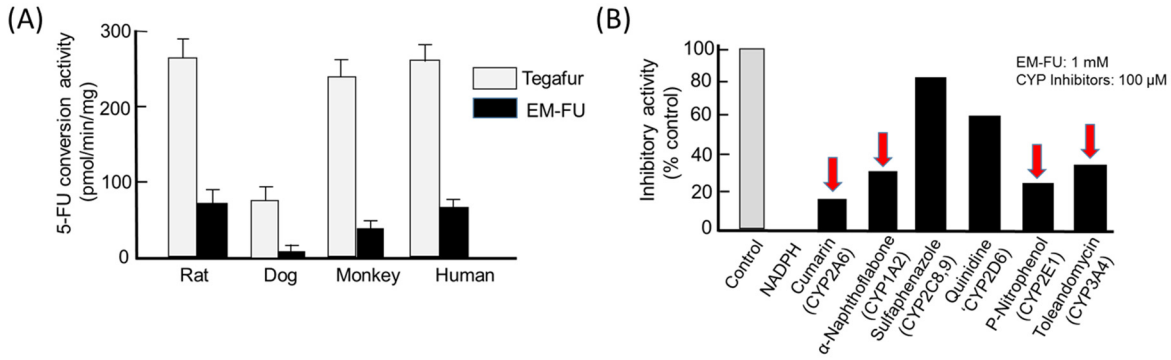

Figure 3.6. Conversion of EM-FU, a major metabolite of DFP-11207, to 5-FU by various liver microsomes.

EM-FU (1 mM) derived from DFP-11207 and FT as a positive control were incubated for 60 min with liver microsomes (0.85 mg proteins) from different origins, and 5-FU produced in the reaction mixture was detected using HPLC system (**A**). The reaction was assayed triplicate. Also EM-FU (1 mM) was incubated with human liver microsomes in the presence of 100 μM coumarin, α-naphthoflavone, sulfaphenazole, quinidine, *p*-nitrophenol, and toleandomycin, respectively, which specifically inhibit corresponding CYP activity (**B**). Data represent mean values ± SD for triplicate assays (**A**) and mean values for duplicate assays (**B**), respectively.

3.3.5 Blood and tissue levels of CTA and 5-FU in tumor-bearing rats after oral administration of DFP-11207.

DFP-11207 (53.4 mg/kg) was orally given to AZ521 tumor-bearing rats and the

distribution of CTA and 5-FU in the blood, tumor and small intestine was investigated. As presented in Figure 3.7.A, CTA was mainly retained in the small intestine (C_{max}; ~100 ng/g tissue) and persisted longer over 12 hours than that in the blood (C_{max}; 32 ng/mL) and AZ521 tumor (C_{max}; below 5 ng/g tissue). At 4 hours following administration of DFP-11207, the levels of 5-FU in the blood and tissues were compared with that of CTA. As show in Figure 3.7.B, 5-FU levels in the blood and tumor were much higher than CTA, suggesting little effect of CTA on the 5-FU phosphorylation to exhibit its antitumor activity in the tumor. In striking contrast, almost equal level of 5-FU and CTA remained in the small intestine. This may well explain with the selective inhibition of 5-FU phosphorylation in the digestive tract resulting in little or no GI toxicity in those rats.

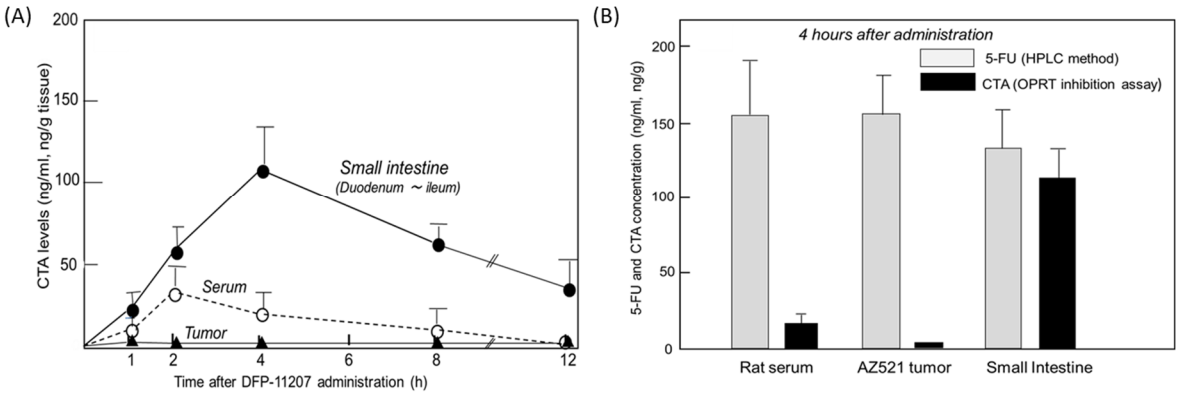

Figure 3.7. CTA and 5-FU levels in blood, small intestine, and tumor tissues of rats after oral administration of DFP-11207.

DFP-11207 (53.4 mg/kg, 75 μmol/kg) was administered to human tumor (AZ521)-bearing xenograft in nude rats. After 1, 2, 4, 8 and 12 h, rats were sacrificed and their blood (as serum), small intestines and tuumors were isolated to prepare the crude extracts containing CTA (**A**) and 5-FU (**B**).
For this, tissues were homogenized with 10 mM potassium phosphate-buffered saline (pH 7.2) and then centrifuged at 9,000x *g* for 30 min. The resultant supernatants (one volume) were treated with four volumes of ethylacetate for 10 min, and obtained organic layer was dried at 40℃. The dried product was dissolved into a small volume of 10 mM phosphate-buffered saline and aliquot of the preparation was applied to HPLC system to measure the concentration of 5-FU and CTA. Data represent mean values ± SD for three rats.

3.3.6 Comparative 5-FU concentration in blood of rats after administration of DFP-11207 and FT-based prodrug S-1.

To distinguish the difference of PK profile between DFP-11207 as the single molecule and S-1 as the cocktail formulation with 1 M FT, 0.4 M gemeracil, and 1 M oteracil, an equimolar amount of DFP-11207 and S-1 (both 50 μmol/kg) was orally given to rats and their plasma 5-FU levels were analyzed.

As shown in Figure 3.8, DFP-11207 had significantly different PK profile from S-1 with low C_{max}, longer T_{max}, and $T_{1/2}$ values although the total AUC with 5-FU from S-1 was two-fold higher than that from DFP-11207 due to a high spike C_{max} of 5-FU from S-1. The desired PK profile with DFP-11207 simulates the 5-FU level in plasma by CI of 5-FU and may well be resulted in the low incidence of myelosuppression by DFP-11207.

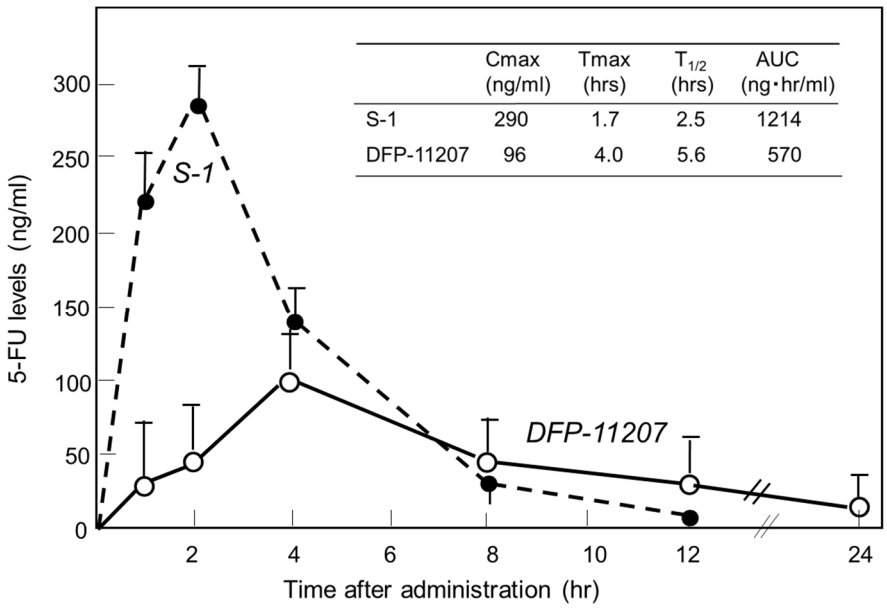

Figure 3.8. Comparative 5-FU levels in rat plasma following oral administration of DFP-11207 and S-1.

A total of 50 μmol/kg of DFP-11207 and S-1 were orally administered to rats (N=3) weighing ~200 g. At indicated time, the blood was isolated and 5-FU levels in the blood were comparatively determined by HPLC. Values are means ± SD for 3 rats.

3.3.7 Antitumor activity of DFP-11207 compared with other antimetabolites on GI cancer xenografts in nude rats.

Antitumor activity of DFP-11207 was further evaluated in human colorectal (HT-29), gastric (MKN-45), and pancreatic (BxPC-3 and Panc-1) cancer xenografts in nude rats, and compared its efficacy with 5-FU (ip) or gemcitabine (intravenous [iv]) using maximum safety doses of the standard care drugs without severe decrease in body weights. As summarized in Figure 3.9 and Table 3.2, DFP-11207 showed significantly higher antitumor activity with ~ 50-65% of tumor growth inhibition (TGI) against HT-29, MKN-45, and BxPC-3 tumor models compared with ~ 30% TGI by 5-FU and gemcitabine, while both DFP-11207 and gemcitabine showed a lower activity, 27% versus 23% in the PANC-1 tumor model. These results strongly support the notion that DFP-11207 can be a new version of clinically development candidates of 5-FU derivatives for the treatment of human GI cancers without a burden of commonly seen side effects including GI toxicity and bone marrow suppression by current standard care drugs, such as 5-FU and gemcitabine.

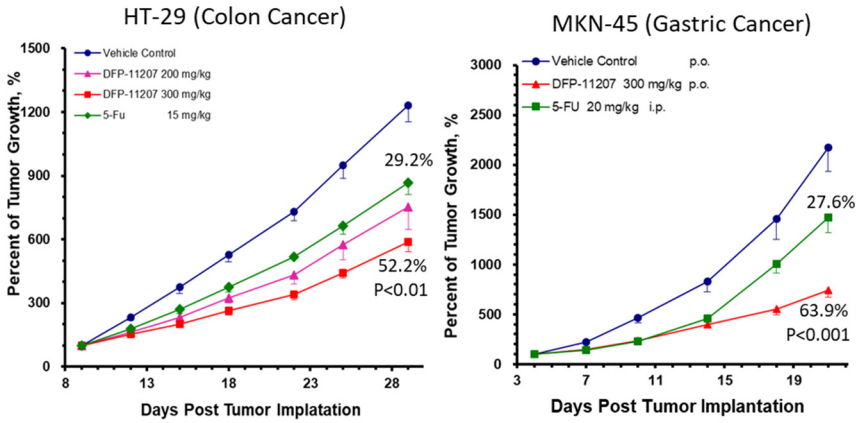

Figure 3.9. Antitumor activity of DFP-1207 compared with 5-FU on human gastrointestinal tumor xenografts in nude rats.

DFP-11207 was orally administered once daily for 14-21 days, 5-FU was intraperitoneally injected daily for 5 days.

Table 3.2. Antitumor activity of DFP-1207 compared with 5-FU or gemcitabine on human gastrointestinal tumor xenografts in nude rats.

Xenografts	Drug	Dose (mg/kg)	Tumor volume (mg/kg)	TGI (%) (mm^3 ±SD)	*p* value
HT-29 (CRC)	Vehicle (0.5% HPMC)		1710±85		
	DFP-11207	300	819±54	52.2	*p<0.01 vs 5-FU*
	5-FU, *ip*	15	1211±76	29.2	
MKN-45 (GC)	Vehicle (0.5% HPMC)		2403±166		
	DFP-11207	300	868±70	63.9	*p<0.001 vs 5-FU*
	5-FU, *ip*	20	1740±70	27.6	
BxPC3 (PC)	Vehicle (0.5% HPMC)		807±51		
	DFP-11207	300	323±29	60.0	*p=0.001 vs Gem*
	Gemcitabine	50	539±37	33.2	
PANC-1 (PC)	Vehicle (0.5% HPMC)		1708±92		
	DFP-11207	300	1243±28	27.2	*NS vs Gem*
	Gemcitabine	50	1320±27	22.7	

Human tumor cells (5 x 10^6 cells) were inoculated into the right axilla of nude rats. When each tumor volume reached ~ 100-200 mm^3, DFP-11207 was orally administered once daily for 14-21 days, 5-FU and gemcitabine were intraperitoneally injected daily for 5 days and weekly for 3 weeks, respectively. Antitumor activities of the drugs were evaluated at day 29 for HT-29, day 21 for MKN-45, day 45 for BxPC3 and day 31 for PANC-1 after tumor implantation.

3.3.8 Comparative antitumor and toxic effects of DFP-11207 and S-1 on human tumor xenografts in nude rats.

Antitumor activity and toxicity represented by the body weight change, visible diarrhea, and change of hematological parameters (white blood cell [WBC], red blood cell [RBC], and platelet [PLT]) were evaluated in KM12C tumor-bearing nude rats after administering equimolar doses of DFP-11207 and S-1 (both 75-112.5 μmol/kg) once daily and 14-day consecutive administration as shown in Figure 3.10.A to 3.10.D.

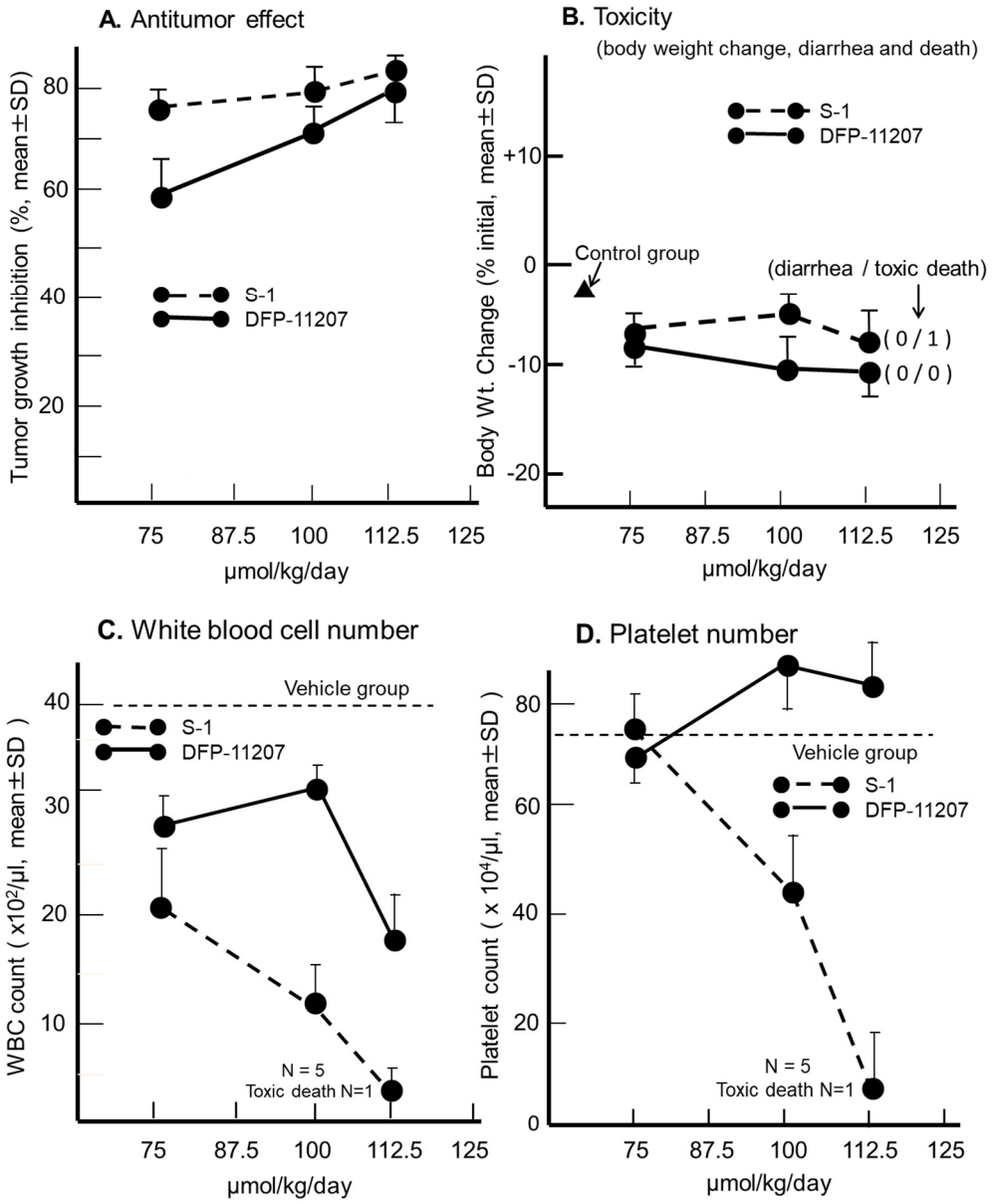

Figure 3.10. Antitumor activity and toxicity of DFP-11207 and S-1 in human colorectal cancer KM12C xenografts in nude rats.

Seventy-five to 112.5 μmoles/kg of DFP-11207 and S-1 were orally administered to KM12C-bearing nude rats (six rats/group) once daily for 14 consecutive days, and antitumor effect (**A**), body weight changes (**B**) and the change of hematological parameters (WBC, (**C**) and platelet count (**D**)) were evaluated. Values are mean ± SD for six nude rats.

Both DFP-11207 and S-1 at 100-112.5 μmol/kg showed a similar and potent inhibition of the tumor growth (Figure 3.10.A) without a significant decrease in body weights (Figure 3.10.B). However, in S-1 group, one out of six rats died after last administration of the drug, suggesting that a hematological change but not GI damage might occur in S-1 group as further described in Figure 3.10.C and 3.10.D. Figure 3.10.C and 3.9.D shows the significant decrease in WBC and PLT counts in S-1 groups while little or no change in the PLT number with a mild decrease in WBC number at the highest dose is evident in DFP-11207 groups. In this pharmacology experiment, no diarrhea was noticed in rats treated with the highest dose of both DFP-11207 and S-1 by the cage-side observation. However, to confirm the evidence of no GI damage in drug-treated rats, a portion of the duodenum was evaluated histochemically as shown in Figure 3.11.

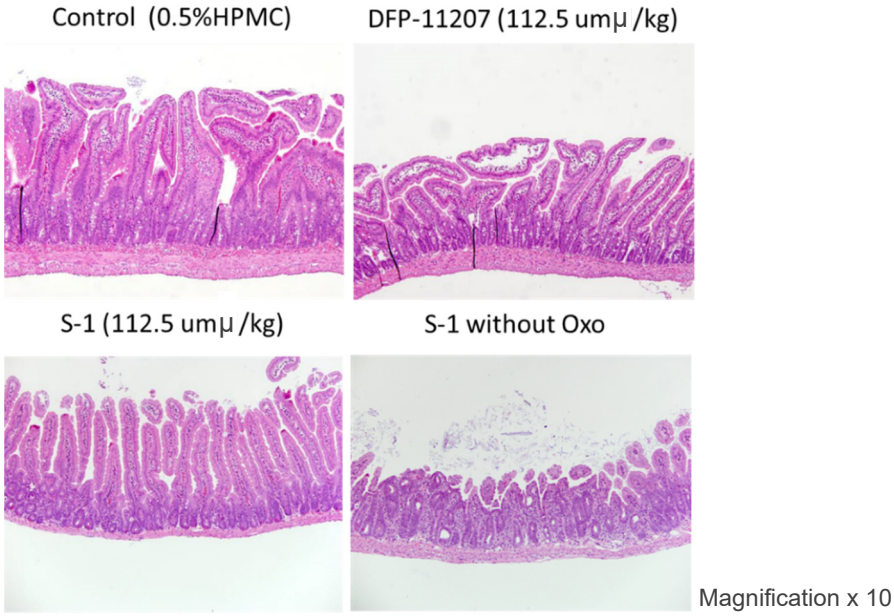

Figure 3.11. Histopathological evaluation of GI tissues (jejunum) in rats treated with each 112.5 μmol/kg of DFP-11207 and S-1.

Portions of the jejunum in rats treated with DFP-11207 and S-1 respectively were isolated and evaluated pathologically by H&E stain. As control group showing 5-FU-induced GI damage, tegaful plus gimeracil alone was administered to rats as same way.

Both DFP-11207 and S-1 did not cause a severe damage of mucosal cells in the GI tract while tegaful plus gimeracil alone (S-1 without oteracil) induced the damage of mucosal layer as show in the right bottom panel. In another pathological study, tegaful plus gimeracil without oteracil has also resulted in 5-FU-induced the GI damage as reported previously[28]. These findings suggest that CTA released from DFP-11207 in the GI mucosal cells prevent the risk from the 5-FU-induced GI toxicity through its inhibition of 5-FU phosphorylation.

3.4 Discussion

For over 50 years, 5-FU has been playing a critical role in the systemic chemotherapy for patients with various cancer types, especially GI cancers. However remarkably different from other cytotoxic drugs, 5-FU exerts its antitumor activity and also toxic effect through an intracellular metabolism to form its active nucleotide, 5-fluoro-2'-deoxyuridine monophosphate (FdUMP) which inhibits the activity of thymidylate synthase (TS) and subsequently inhibits the biosynthesis of DNA in tumor or rapid-growing normal cells. However, 5-FU is rapidly degraded to inactive catabolites by DPD in the liver and interestingly, resultant hydrolysates from 5-FU have been suggested resulting in adverse events, such as cardiotoxicity, neurotoxicity and skin-toxicity to patients. Also it has been well known that 5-FU-induced efficacy and toxicity are altered by clinical doses and cumulative schedules of 5-FU to cancer patients[20]. Considering such *in vivo* events of 5-FU in cancer patients, it is an urgent unmet medical need to develop a novel 5-FU derivative which provides a maximal antitumor activity of 5-FU with less adverse events in patients. On the viewpoint of such thought, previously Shirasaka *et al* developed S-1, the oral combination drug consisting of 1 M tegafur (prodrug of 5-FU),

0.4 M gimeracil (inhibitor of DPD), and 1 M oteracil (OPRT inhibitor), with protection of GI toxicity[23, 31]. Due to the nature of a cocktail formulation, each component in S-1 exhibits independent PK profile, respectly. Especially the higher C_{max} level of 5-FU derived from tegafur in the blood resulted in hematological and/or GI toxicities in patients for a long-term use[26, 32]. Accordingly, it is desired to have 5-FU level in blood maintained for a long-time at a relatively low C_{max} level for a new oral candidate of fluoropyrimidine derivatives.

Based on the past pre-clinical and clinical experiences to pharmacological and PK properties of 5-FU and its oral prodrugs, we newly developed a conceptual oral 5-FU derivative with self-controlled toxicity, DFP-11207 (Figure 3.1.). DFP-11207 consists of three important chemical components, EM-FU, CDHP, and CTA as a single molecule. As expected, DFP-11207 protected the 5-FU-induced GI track, hematological, cardiac and neuro toxicities and HFS with favorable PK profiles, the low C_{max} and long half-life in the plasma 5-FU level. To ensure that these components in DFP-11207 work each other to attain a functional role, I and my colleagues investigated enzymatic hydrolysis and inhibitory activity in both 5-FU-degradation and phosphorylation enzymes *in vitro*, inhibitory effect on the intracellular phosphorylation and subsequent metabolism of 5-FU in intact cells, and a metabolism in liver microsomes (CYP species). As shown in Figure 3.3 and Table 3.1, DFP-11207 was found to be rapidly hydrolyzed to produce EM-FU, CDHP and CTA, and strongly inhibit both DPD and OPRT activities in cell-free system using rat plasma and 20% homogenates of the rat liver and small intestine. Especially, their inhibitory activity of DFP-11207 in DPD and OPRT was almost equivalent to those by CDHP and CTA alone[28, 33]. However it is necessary to confirm whether DFP-11207 inhibit an intracellular phosphorylation and subsequent metabolism of 5-FU in intact cells

because of no inhibition by CTA alone for the intracellular phosphorylation of 5-FU as reported previously.[28] As presented in Figure 3.3, only DFP-11207 did inhibit dose-dependently the intracellular metabolism of 5-FU in intact tumor cells, suggesting a possible inhibition of 5-FU phosphorylation by CTA produced in GI mucosal cells after an oral administration of DFP-11207. Unfortunately I and my colleagues could not confirm such intracellular inhibition by DFP-11207 using innate normal mucosal cells due to the technical challenge for a stable isolation of mucosal cells from intact GI tissues. Therefore, I and my colleagues investigated the distribution of CTA and 5-FU in GI tissues in tumor-bearing rats followed by an oral administration of 53.4 mg/kg DFP-11207 to ensure whether CTA derived from DFP-11207 inhibits the intracellular phosphorylation of 5-FU (formation of 5-fluoronucleotides) which is sufficient to induce GI injury including diarrhea. As shown in Figure 3.6.A, CTA was found to be mainly retained in GI tissues compared with that in plasma and tumor tissues. Furthermore, 5-FU levels were almost same to the CTA level in GI tissues while 5-FU was highly distributed in the plasma and tumors. The results strongly support the notion that CTA protects the incidence of GI injury via the inhibition of 5-FU phosphorylation without compromising the antitumor activity by 5-FU (Figure 3.6.B).

As described above, EM-FU is a prodrug and shows the antitumor activity by its active form, 5-FU. However, an active 5-FU was not produced from EM-FU in a 20% tissue homogenate system, suggesting the formation of 5-FU from EM-FU by drug-metabolizing enzymes (namely microsomes) in the liver. And I and my colleagues confirmed that EM-FU was specifically hydrolyzed to 5-FU by various CYP subtypes (CYP 1A2, 2A6, 2E1 and 3A4) as shown in Figure 3.4 although microsomal activation rate of EM-FU was lower than that by tegafur. In the case of tegafur, it has been reported

to be activated by only CYP 2A6[34].

It has been demonstrated in clinical studies that the efficacy and toxicity of 5-FU depend on its concentration and duration time in the blood of patients[20], and recently, Lee *et al* have proposed the importance for therapeutic drug monitoring of 5-FU to maximize its efficacy and to reduce 5-FU-induced adverse events in their review article[35]. DFP-11207 is the oral prodrug of 5-FU minimizing the 5-FU-induced toxicities without compromising its antitumor activity. The desired feature is different from that by the iv 5-FU or other oral 5-FU prodrugs and supported by its favored PK profile of plasma 5-FU following administration of DFP-11207 to rats. I and my colleagues measured 5-FU levels in the blood and compared with that after the administration of another oral prodrug S-1, possessing the product from a similar drug concept. As shown in Figure 3.6., DFP-11207 resulted in lower C_{max} and AUC values but longer T_{max} and $T_{1/2}$ values of 5-FU, respectively than S-1, which suggests that DFP-11207 would be superior to avoid the 5-FU-induced severe hematological toxicity including neutropenia, in particular, thrombocytopenia on the top of the protection of 5-FU-induced GI toxicities.

In pharmacology study with S-1 in a site-by-site comparison, DFP-11207 showed an antitumor activity in a dose-dependent manner without loss of host body weights or pathological GI damages as same as S-1. However, DFP-11207 resulted in a mild WBC count decrease at a higher dose but no effect on the PLT number, whereas the hematological toxicities were evident with the treatment with S-1. Although the mechanism remains to be cleared, the desired PK profile of DFP-11207 as described above may well contribute to the advantage over S-1 for the bone marrow effect that could be a good benefit for a population of patients who is prone to and compromised with bone marrow suppression or recovery.

Regarding to 5-FU-induced cardiotoxicity and/or neurotoxicity, it has been speculated that the catabolites of 5-FU would contribute to an incidence of those toxicities. In safety pharmacology study of DFP-11207, it showed no neurotoxicity in rats and no cardiovascular toxicity in cynomolgus monkeys (data not shown), suggesting that inhibition of 5-FU degradation may be concerning to decrease in the incidence of such toxicities.

Cumulative dosage and schedule of 5-FU in combination with other cytotoxic drugs are variable in clinical setting to treat patients with GI cancers; bolus injection of 5-FU is applied in FP regimen for advanced gastric cancer, and both 46-hour continuous and sequential bolus injection of it are used in FOLFOX and FOLFIRI regimens for metastatic colorectal cancer. However, these combination regimens certainly accompany severe adverse events for most patients although the therapeutic response assessed by response rate, progression-free survival, and overall survival. The advantage of DFP-11207 such as self-controlled toxicity sheds light on a new potential applied to clinical setting and combined with other cytotoxic drugs to improve QOL in cancer patients and for long survival of patients.

Phase I study of oral DFP-11207 has finished to evaluate adverse events and PK profile of this drug. A preliminary result has suggested that DFP-11207 is well tolerated and no severe drug-limiting toxicity including severe diarrhea and thrombocytopenia. It is hopeful to have a further clinical investigation to confirm the advantage of DFP-11207 in pre-clinical settings.

Chapter 4 Practical Research of Novel Deoxycytidine Analog, DFP-10917

4.1 Introduction

Antitumor nucleosides, particularly the deoxycytidine analog (Figure 4.1), are key anticancer drugs which play an important role in the treatment of patients with solid tumors and leukemia. For instance, gemcitabine (GEM) and cytosine arabinoside (cytarabine) have been clinically used as a standard of care treatment in patients with pancreatic and non-small cell lung cancers[36-38], as well as in patients with and acute myeloid leukemia (AML)[39-43]. A well-accepted cytotoxic mechanism of these drugs involves the inhibition of DNA biosynthesis through their incorporation into DNA molecules or the inhibition of DNA polymerases following the conversion to their tri-phosphate forms in cancer cells. However, these drugs are rapidly inactivated by the cytidine deaminase in normal and tumor tissues[43]. Accordingly, relatively high doses of these drugs via bolus injection is common clinical practice in patients to avoid such an inactivation; 1,000-1,500 mg/m^2 of GEM and 2-3 g/m^2 of cytarabine as induction therapy are frequently administered to patients with pancreatic cancer and AML, respectively.

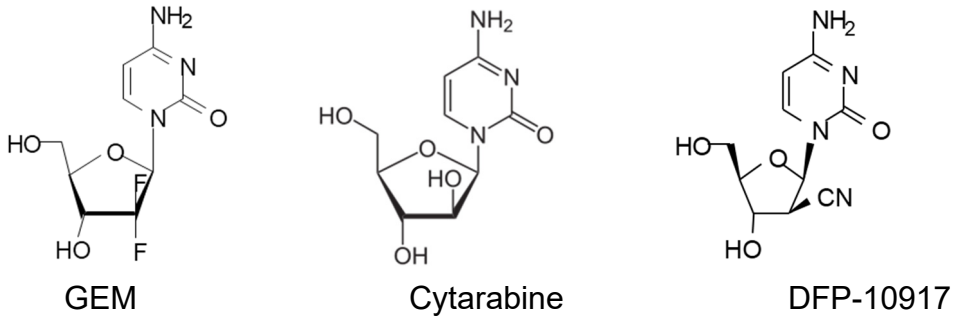

Figure 4.1. Molecular structure of deoxycytidine analog.

GEM, gemcitabine; Cytarabine (cytosine arabinoside); DFP-10917, 2'-C-Cyano-2'-deoxy-1-β-D-arabino-pentofranocylcytosine (formerly abbreviation: CNDAC).

2’-C-Cyano-2’-deoxy-1-β-D-arabino-pentofranocylcytosine (DFP-10917, formerly CNDAC) was developed in the early 1990s as a deoxycytidine analog (Figure 4.1)[44, 45], which has shown potent antitumor effects on various murine and human tumors *in vitro* and *in vivo*[46]. Similar to other cytidine nucleosides, such as GEM and cytarabine, DFP-10917 has been demonstrated to be efficiently phosphorylated to its mono-, di- and tri-phosphate forms and is incorporated into the DNA of tumor cells *in vitro*[47]. As regards the behavior of the triphosphate form of DFP-10917, following incorporation into DNA, Hayakawa *et al* speculated that it would chemically terminate an enzymatic DNA-chain elongation[48] and for this, there are some supporting data that DFP-10917 induces DNA double-strand breaks (Figure 4.2) and G2 cell cycle arrest in tumor cells *in vitro*[49-53]. On the other hand, a major functional mechanism of GEM and cytarabine has been estimated to be the direct inhibition of DNA polymerases, rather than their incorporation into DNA in tumor cells, affecting DNA synthesis[54-56].

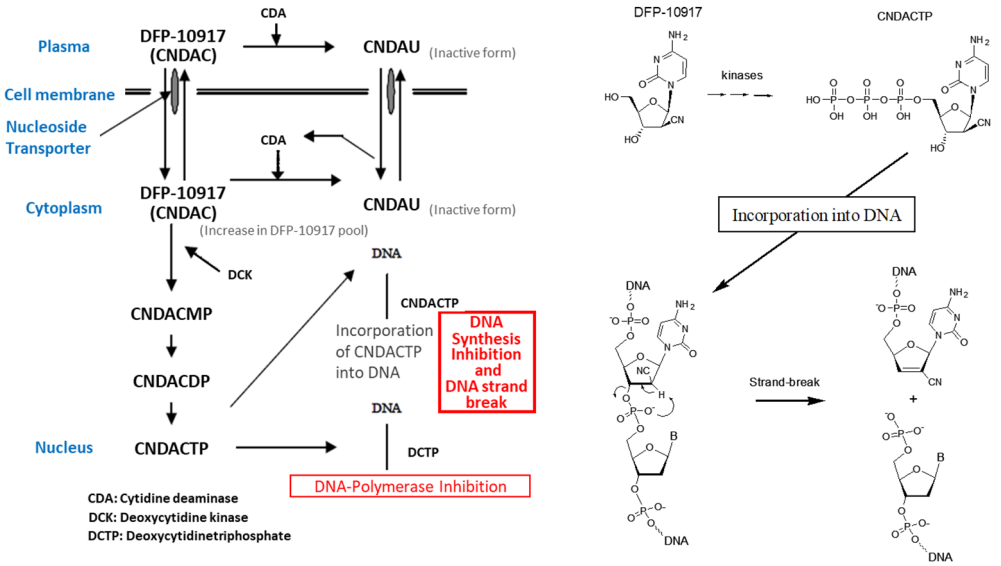

Figure 4.2. A possible DNA strand-break mechanism of DNA containing DFP-10917[50].

CNDAC, DFP-10917; CNDACTP, CNDAC 5’-triphosphate; CNDAU, 2'-cyano-2',3'-didehydro-2',3'-dideoxyuridine.

However, such reports mentioned above, including those on GEM, cytarabine and DFP-10917, have focused on the clarification of their drug-induced functional mechanisms in tumor cells *in vitro*. However, the exact clinically available treatment regimen using these compounds which would prove to be most effective for cancer patients remains to be established. In addition, the functional mechanisms related to the drug schedule need to be elucidated.

The aim of this research is to develop the unique functional mechanism *in vivo* for the active substance, DFP-10917, which it cause the DNA double-strand and G2/M cell cycle arrest *in vitro*. For this purpose, this research is conducted the comparison with the previous studies and the existing drug focused on the three factors, which they perform the conversion from high dose and short time to low dose and long periods as the administration (one of the module), the adoption of continuous infusion as the route (one of the module), and the selection of hematological cancer as the disease (one of the module), based on the *in vitro* unique mechanism and antitumor activity of DFP-10917 as module drug discovery. In addition, the association between the dose intensity with the dosing schedule by using the human tumor xenograft models and other analysis methods is aimed to confirm, and the novel functional mechanisms of DFP-10917 compared to other deoxycytidine analogs are elucidated *in vivo*.

4.2 Materials and methods

4.2.1 Chemicals

DFP-10917 (CNDAC) was manufactured by Delta-Fly Pharma, Inc. (Tokushima, Japan). Cytosine arabinoside (cytarabine) and gemcitabine (GEM) were purchased from Sigma-Aldrich Inc. (St. Louis, MO, USA). Paclitaxel and cisplatin (CDDP) were

purchased from Wako Pure Chemical Industries, Ltd. (Osaka, Japan). Decitabine, an inhibitor of DNA methyltransferase, was kindly provided by Otsuka Pharmaceutical Co. Ltd. (Tokyo, Japan). The comet assay^{TM} kit was obtained from Trevigen Inc. (Gaitherburg, MD). All other chemical and biochemical materials were commercial products.

4.2.2 Tumor cells

The human MV-4-11 and CCRF-CEM leukemia cells, and the U937 lymphoma cells were purchased from Dai-Nippon Sumitomo Pharmaceutical Co. Ltd. (Osaka, Japan). The human colon cancer KM20C cells, lung cancer Lu-99 and Lu-61 cells were obtained from JCRB Cell Bank (National Institutes of Biomedical Innovation, Health and Nutrition, Japan). The human pancreatic cancer PAN-4 cells were obtained from the Central Institute for Experimental Animals (Kawasaki, Japan). Although the KM20C cells are considered to have been contaminated and are mixed rectosigmoid adenocarcinoma cells, and the data regarding the PAN-4 cells has not been disclosed, I and my colleagues decided to use these cells in our study, as it was considered that this contamination and these undisclosed data would have no influence on the comparative experiments. Human cervical cancer HeLa cells were obtained from ATCC (The Global BioSource Center, Manasas, VA, USA). The SKOV-3 human ovarian cancer cells were kindly provided by Dr. Mitsuaki Suzuki at Jichi-Medical University (Tochigi, Japan). These tumor cells were cultivated and maintained in RPMI-1640 medium containing 10% fetal bovine serum. Human solid tumor xenografts were prepared by the serial implantation of cells *in vitro* into the right axilla of nude mice at 3-week intervals until analysis.

4.2.3. Animals

A total of 135 male BALB/cA Jcl-nu mice and 190 male C.B-17/Icr-scid Jcl mice (5 weeks old, weighing 17.2-24.6 g), were purchased from KREA Japan Inc. (Tokyo, Japan) and maintained on a commercial diet and autoclaved water, made available *ad libitum*. The care and treatment of the animals were in accordance with the guidelines issued by the Science and International Affairs Bureau of the Japanese Ministry of Education, Science, Culture and Sports. The experimental protocol was carried out following the approval of the Institutional Animal Ethical Committee at the research facility of Delta-Fly Pharma, Inc.

4.2.4. Antitumor experiments

Groups of 6 or 7 nude mice were used. The KM20C, Lu-99, MV-4-11 and U937 tumor xenografts were prepared, respectively, by the subcutaneous implantation (~ 2x2 mm fragments of tumor slices) into the right axilla of BALB/cA Jcl-nu mice. When the tumor volume reached ~ 200 mm^3, DFP-10917 (30, 8 or 4.5 mg/kg/day) was continuously infused by an Alzet osmotic pump for 24 consecutive hours on days 1 and 8, for 3 consecutive days on days 1 and 15, or for 14 consecutive days, or DFP-10917 (500 mg/kg/day) was administered via bolus injection on days 1 and 8. Cytarabine (100 mg/kg) was administered via intravenous (iv) injection on days 1-5 and days 8-12, and GEM (300 mg/kg) was administered via iv injection on days 1 and 8. Following drug treatment, the condition of the mice was monitored daily for 30 days. The longest tumor diameter formed by the KM20C cells was 18.51 mm and the maximum tumor volume was 2750.75 mm^3. None of the mice developed multiple tumors. The tumor volume [1/2 x (the major axis) x (the minor axis)^2] was measured twice a week throughout the treatment period (14

days), and the relative tumor volume (RTV) was calculated as follows:

RTV = (mean tumor volume during therapy)/(mean tumor volume at the start of therapy).

The antitumor effects of DFP-10917, cytarabine and GEM were estimated by the following equation: Mean inhibition rate of tumor growth (IR, %) =

[1 -(mean RTV of drug-treated group/mean RTV of control group) x100].

4.2.5 Survival experiments

For the U937 lymphoma cells, groups of 10 C.B-17/Icr-scid Jcl mice were used. Prior to tumor cell implantation, 0.2 ml of anti-mouse Asialo GM1 antibody [antibody to natural killer (NK) cells] was injected intraperitoneally into all mice. The following day (day 1), the U937 lymphoma cells ($1x10^7$ cells /0.5 ml/mouse) were implanted into the intraperitoneal (ip) cavity of the mice. From day 2, DFP-10917 (4.5 mg/kg/day) was continuously infused for 14 days, cytarabine (100 mg/kg/day) was administered via iv injection on days 3-7 and days 10-14, and decitabine (1.0 mg/kg/day) was administered via ip injection on days 3-5 and days[43-45]. Following drug treatments, the survival of the mice was monitored daily for 90 days. The antitumor activity of the drug was evaluated as the survival effect (ILS, %) by the following equation:

ILS (%) = [mean survival days in drug-treated group /

mean survival days in control (no treatment) group - 1] x100.

As one of the endpoints, the survival times with the respective agents were comparatively investigated.

For another tumor model using intraperitoneally disseminated ovarian cancer (SKOV-3) cells, the tumor cells ($2x10^7$ cells/0.5 ml/mouse) were implanted, and after 24 h of implantation the mice (C.B-17/Icr-SCID Jcl) were treated with DFP-10917 (4.5

mg/kg/day, 14 days), GEM (300 mg/kg/day, days 1 and 8), CDDP (7 mg/kg/day, days 1 and 8) and paclitaxel (50 mg/kg/day, day 1) as a positive control under the scheduled time periods.

4.2.6. Evaluation of drug-related toxicity

The body weights of the tumor-bearing mice were measured as an index of drug-induced toxicity, and the rate (%) of changes in body weight (BWC) was calculated by the following equation: BWC (%) =

[(body weight on day n) - (body weight on day 0)] / (body weight on day 0) x100. The maximum body weight of the mice with tumors derived from the Lu-99 cells was 25.0 g at the beginning of the experiment and 29.9 g upon sacrifice.

4.2.7 Comet assay

According to the manual provided with the Comet assay kit[57], the drug-treated cells were fixed on a glass slide, and treated with lysis solution for > 1 h. The slide glass containing the drug-treated cells was then moved to an electrophoresis instrument and the cells were exposed to 33 V and 300 mA electrophoresis for 20 min, and then soaked in 0.4M Tris-HCl buffer (pH 7.5) for approximately 10 min. This procedure was repeated once more. After soaking in 70 % ethanol for 5 min, the glass slide was dried to yield a thin-layer film. Finally, 50 µl aliquots of ethidium bromide solution (20 µg/ml) were dropped onto the glass slide. After a coverglass was placed on the glass slide, the migration rate of the drug-treated cells (50 cells) was observed with an analysis apparatus for Comet assay.

4.2.8 Evaluation of DNA fragmentation

The drug-induced fragmentation of DNA in the CCRF-CEM cells was evaluated by the rate of electrophorated DNA (%tail DNA) and olive tail moment calculated by the following equation: Olive tail moment = (tail.mean - head.mean) x %tail DNA/100.

4.2.9 Cell cycle analysis

The HeLa cells ($1x10^6$) were inoculated into 6-well plates and treated with either 1 to 30 μM of DFP-10917 or 0.03 to 0.3 μM of GEM. Untreated cells were used as the control group. Viable cells were counted 24, 48 and 72 h after the inoculation to analyze the effects of the drug on cell cycle progression using a commercially available cell-cycle analyzer, FACS Calibur flow cytometer (Becton-Dickinson, Franklin Lakes, NJ, USA).

4.2.10 Statistical analysis

The significance of differences between groups with or without drug treatment was assessed using the generalized Wilcoxon test. A value of $P<0.05$ was considered to indicate a statistically significant difference.

4.3 Results

4.3.1 Effect of infusion time on the antitumor activity of DFP-10917 *in vivo*

It is well known that the dosing schedule of drugs influences their antitumor activity and has adverse events on cancer patients[58, 59]. In a preliminary experiment using KM20C tumor-bearing mice to determine the maximum tolerance dose (MTD) of DFP-10917 at various doses and administration schedules without death and a -20% change in body weight, it was found from the result that the MTD was thus determined to be 500

mg/kg/day for iv bolus injection on days 1 and 8, 30 mg/kg/day for 1-day continuous infusions on days 1 and 8, 8 mg/kg/day for 3-day continuous infusions on days 1 and 15, and 4.5 mg/kg/day for 14-day continuous infusion (data not shown). Based on the results, the antitumor activity and toxicity of the infusion time of DFP-10917 on the same KM20C human cancer xenografts in nude mice was evaluated. As shown in Figure 4.3.A, no re-growth of tumors or body weight loss were observed during days 15-29 following the initiation of treatment with DFP-10917 for the 14-day continuous infusion schedule (4.5 mg/kg) compared to the other schedules [iv bolus injection (500 mg/kg, days 1 and 8), 1-day continuous infusion (30 mg/kg, days 1 and 8), and 3-day continuous infusion (8 mg/kg, days 1 and 15)]; the prolonged (at least over 7 days) administration of DFP-10917 at a low dose of 4.5 mg/kg/day resulted in the most potent antitumor activity with an >70% inhibition of tumor growth (IR) compared to its shorter (1 to 3 days) administrations. These results thus suggest that in order to achieve the maximal response against human cancers, DFP-10917 should be administered by long-term infusion (14 days) at a lower dose (4.5 mg/kg).

4.3.2 Re-growth rates of colon tumors following treatment with DFP-10917 in various dosing schedules.

In the same antitumor experiment, the re-growth rates of KM20C tumors on days 15, 22 and 29 after the infusion of DFP-10917 with the 1- to 14-day schedules were observed. As shown in Figure 4.3.B, the IR of tumor growth after a 1-day infusion with high-dose (30 mg/kg/day) DFP-10917 significantly decreased from 70.1% (on day 15) to 45.7% on day 29. By contrast, the 14-day infusion of 4.5 mg/kg/day DFP-10917 resulted in an increased IR from 79.6% (on day 15) to 98.6% (on day 29), suggesting that the

prolonged infusion with low-dose DFP-10917 prevented tumor re-growth after the terminated administration.

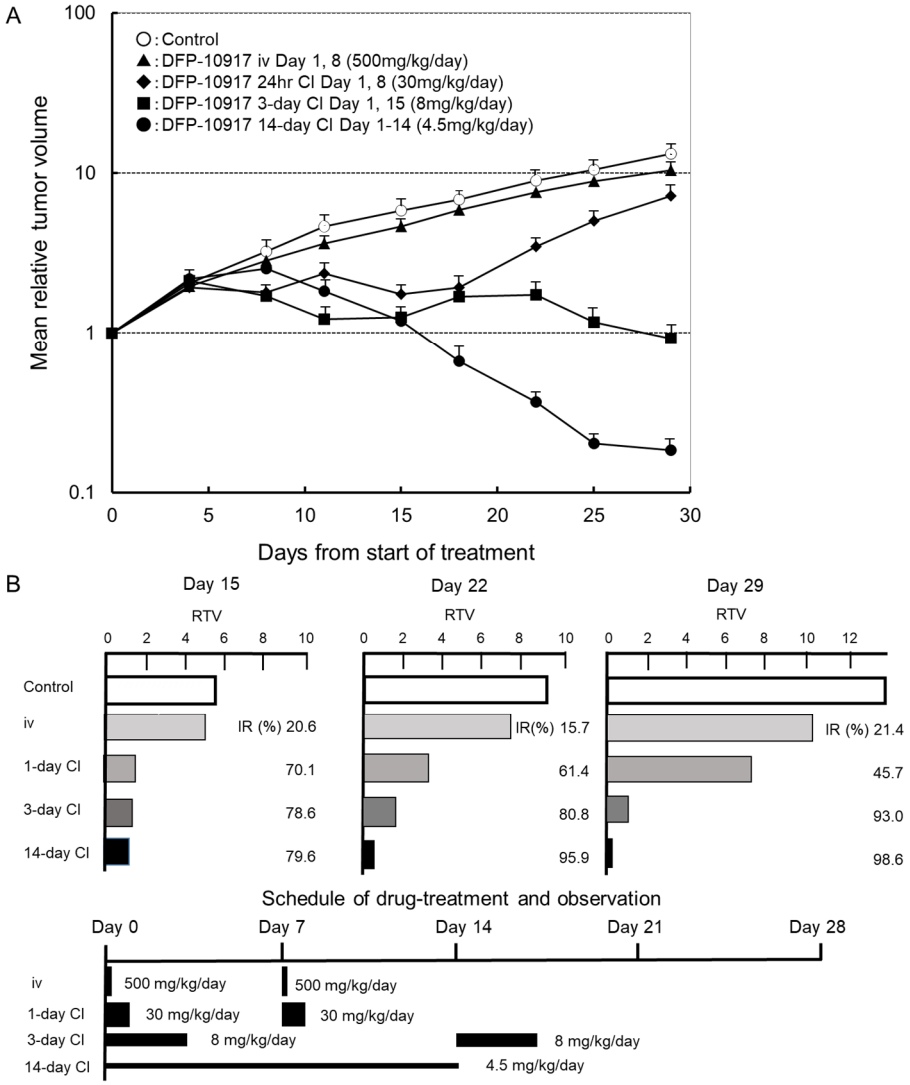

Figure 4.3. Effect of infusion time on the antitumor activity of DFP-10917 in KM20C human tumor xenografts in nude mice.

The MTD dose of DFP-10917 was infused for 1 day (30 mg/kg/day) x2, 3 days (8 mg/kg/day) x2, and 14 days (4.5 mg/kg/day), respectively, to KM20C tumor-bearing mice from 7 days after implantation. Relative tumor volume (RTV) was calculated as follows: RTVn = (TV on day n)/(TV on day 0), n=4, 8, 11, 15, 18, 22, 25 and 29. (**A**) On day 15, the tumor growth inhibitory effects of DFP-10917 were evaluated for each treatment group, and thereafter, (**B**) the regrowth rate of the tumors was measured on days 15, 22 and 29, respectively. Data represent mean values of relative tumor volume for 7 mice.

4.3.3 Effect of the prolonged infusion of DFP-10917 on human lung cancer xenografts.

GEM is mainly used to treat patients with advanced pancreatic and lung cancer as one of the first-line treatment regimens[60, 61]. However, such a treatment is generally ineffective and patients become resistant to this drug[62, 63]. Therefore, there is an urgent need for the development of a novel treatment regimen with which to control the progression of pancreatic and lung cancer. In this study, the efficacy of DFP-10917 in comparison to GEM of one of the deoxycytidine analogs by using Lu-99 human lung cancer xenografts was examined. DFP-10917 was found to control and/or suppress the growth of Lu-99 tumor throughout the therapeutic periods up to 29 days, while GEM exhibited limited efficacy on this tumor, as was expected (Figure 4.4).

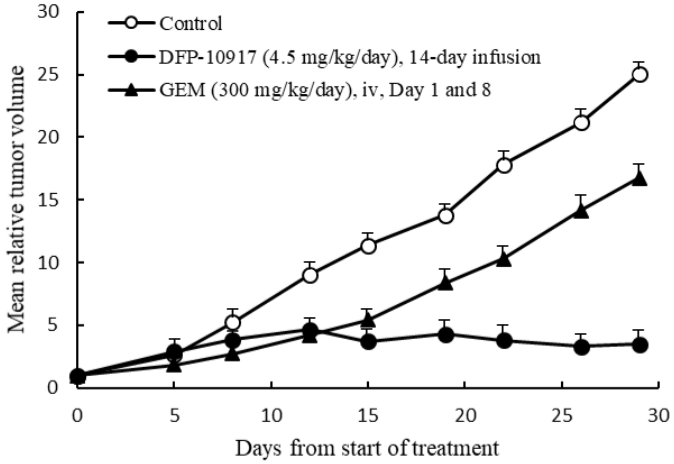

Figure 4.4. Antitumor effect of DFP-10917 and gemcitabine on Lu-99 human lung cancer xenografts resistant to gemcitabine.

In this therapeutic experiment, a low dose (4.5 mg/kg/day) of DFP-10917 was continuously infused for 14 days, and a high dose (300 mg/kg/day) of gemcitabine was administered intravenously (iv) weekly for 2 times. Values are the means ± SD for 6 mice. Relative tumor volume (RTV) was calculated as follows: RTVn = (TV on day n)/(TV on day 0), n=5, 8, 12, 15, 19, 22, 26 and 29.

In separate experiments for comparing DFP-10917 and GEM by using PAN-4 pancreatic and Lu-61 lung cancer xenografts, the same dose rates and treatment schedules for DFP-10917 and GEM resulted in an 84 and 59% IR, respectively in PAN-4-derived tumors, and in 91 and 17% IR, respectively, in Lu-61-dervied tumors (data not shown). Throughout these experiments, the prolonged 14-day infusion of DFP-10917 was suggested to have an antitumor activity comparative to that of GEM.

4.2.4 Effect of the long-term infusion DFP-10917 on hematological tumor cells in mice.

Cytarabine has been a standard of care for the treatment of patients with acute myeloid leukemia (AML). A bolus injection of high doses of cytarabine has been applied due to the rapid inactivation by cytidine deaminase (CDA) and the activation by deoxcytidine kinase (DCK). Thus, the anticancer activity of DFP-10917 and cytarabine in the U937 cells (DCK/CDA=1.6, cytarabine sensitivity) and MV-4-11 cells (DCK/CDA=12.4, cytarabine resistance) tumors was thus comparatively evaluated (solid forms in both cases). As shown in Figure 4.5, the prolonged infusion of DFP-10917 markedly affected both U937 and MV-4-11 tumor xenografts with a 98.8 and 98.7% IR, respectively, compared to treatment with cytarabine which yieled an 83 and 43.6% IR, respectively. It is worth mentioning that DFP-10917 markedly abolished tumor growth over the 14-day therapeutic period.

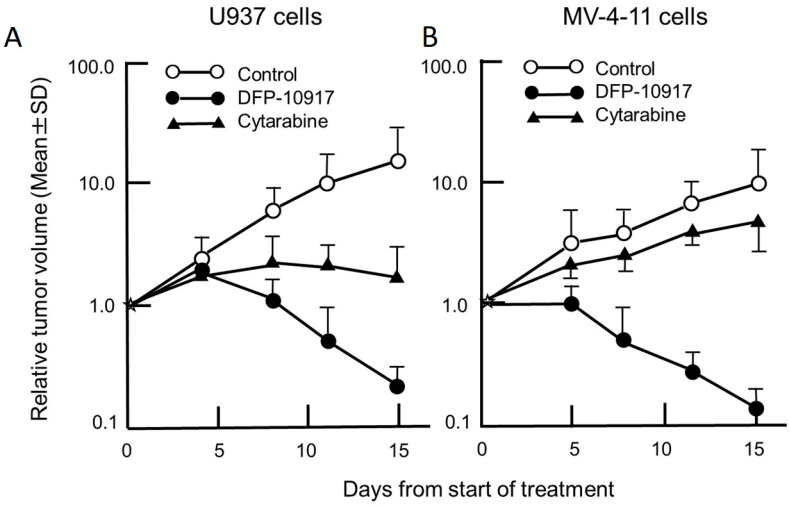

Figure 4.5. Anti-leukemic effect of DFP-10917 and cytarabine on (**A**) U937 and (**B**) MV-4-11 human lymphoma xenografts.

U937 and MV-4-11 cells were inoculated into mice as solid forms for 7 mice, respectively, and 7 days after implantation. DFP-10917 (4.5 mg/kg/day) was infused for 14 days, and cytarabine (100 mg/kg/day) was injected intravenously (iv) on days 1-5 and days 8-12. Relative tumor volume (RTV) was calculated as follows: RTVn = (TV on day n)/(TV on day 0), n=5, 8, 12 and 15.

4.3.5 Comparative survival effect of DFP-10917 on ascitic U937 and SKOV-3 tumor xenografts in mice.

As the ultimate objective of drug treatment in advanced cancers is the achievement of prolonged survival with a good quality of life (QOL), the effects of DFP-10917 by 14-day infusion on survival were examined on ascitic U937 leukemia cells. As shown in Table 4.1, DFP-10917, cytarabine and decitabine led to a 165, 127 and 33% increase in lifespan (ILS), respectively; this suggests a favorable pro-survival effect of DFP-10917 compared with cytarabine and decitabine. The effects of DFP-10917, GEM, CDDP and paclitaxel as standards of care for ovarian cancer, were further evaluated in a disseminated ascitic form of SKOV-3 ovarian cancer cells in mice (Table 4.1). The

prolonged infusion of DFP-10917 was also demonstrated to significantly increase the long-term survival by 234% compared to GEM (12%), CDDP (39%) and paclitaxel (47%). Throughout two therapeutic experiments, the prolonged infusion of DFP-10917 at a low dose clearly prolonged the survival time in both leukemia cells and intraperitoneally disseminated solid tumors, suggesting its potential clinical benefit for patients with cancer.

Table 4.1. Effects of DFP-10917 on the survival of mice with U937 or SKOV-3 human tumor xenografts.

Cell line	Drug	Dose (mg/kg/day)	Treatment	No. of mice	Survival time (days, mean ± SD)	ILS[a] (%)
U937 (lymphoma)	Control	-	-	10	32.9 ± 30.5	-
	DFP-10917	4.5	s.c., days 3-17	10	87.2 ± 6.1[b,c,d]	165.0
	Cytarabine	100	i.v., days 3-7, 10-14	9	74.4 ± 15.5[b]	127.0
	Decitabine	1.0	i.p., days 3-5, 10-12 (bid)	10	43.8 ± 24.7	33.1
SKOV-3 (ovarian carcinoma)	Control	-	-	10	22.0 ± 2.2	-
	DFP-10917	4.5	s.c., days 1-14	10	73.5 ± 4.6[e,f,g,h]	234.1
	Paclitaxel	50	i.v., day 1	10	32.3 ± 7.9[e]	46.8
	CDDP	7	i.v., days 1, 8	10	30.6 ± 4.7[e]	39.1
	Gemcitabine	300	i.v., days 1, 8	10	24.7 ± 1.3[e]	12.3

U937 cells ($1x10^7$cells/0.5 ml/mouse) were implanted into ip cavity of C.B-17/Icr-scid Jcl mice. After 2 days, the mice were treated with the drugs and the survival time of each mouse was then observed for 90 days. SKOV-3 cells ($2x10^7$cells/0.5 ml/mouse) were implanted into the ip cavity of C.B-17/Icr-scid Jcl mice. After 24 h, the mice were treated with the drugs and the survival time of each mouse was observed for at least 90 days. [a]ILS indicates the increase in lifespan. ILS (%) = (mean survival time of treatment group/mean survival time of control group - 1) x100. Significant differences were observed by the generalized Wilcoxon test as follows: [b]Control vs. DFP-10917 ($P<0.005$), bcontrol vs. Cytarabine ($P<0.05$), [c]Cytarabine vs. DFP-10917 ($P<0.05$) and [d]Decitabine vs. DFP-10917 ($P<0.005$). In addition, significant differences were observed by the generalized Wilcoxon test as follows: [e]Control vs. DFP-10917 ($P<0.0001$), [e]Control vs. Paclitaxel ($P<0.0005$), [e]Control vs. CDDP ($P<0.0001$), [e]Control vs. Gemcitabine ($P<0.01$), [f]Paclitaxel vs. DFP-10917 ($P<0.0001$), [g]CDDP vs. DFP-10917 ($P<0.0001$) and [h]Gemcitabine vs. DFP-10917 ($P<0.0001$).

4.3.6 DNA double-strand breaks in human cancer cells following treatment with DFP-10917.

To investigate the cytotoxic mechanisms of the prolonged infusion of DFP-10917 compared to other deoxycytidine analogs, such as cytarabine and GEM, DNA strand-breakage following the continuous exposure to DFP-10917 and cytarabine or GEM was investigated by comet assay[56] in human leukemia CCRF-CEM cells and solid cervical cancer HeLa cells. In the CCRF-CEM cells, 1 μM DFP-10917 (IC_{50} value) induced marked DNA fragmentation with 26.88±12.84 of % tail, while 1 to 10 μM (IC_{50} and IC_{70} values) cytarabine induced limited DNA fragmentation with approximately 6.95±6.65 of % tail DNA (Figure 4.6).

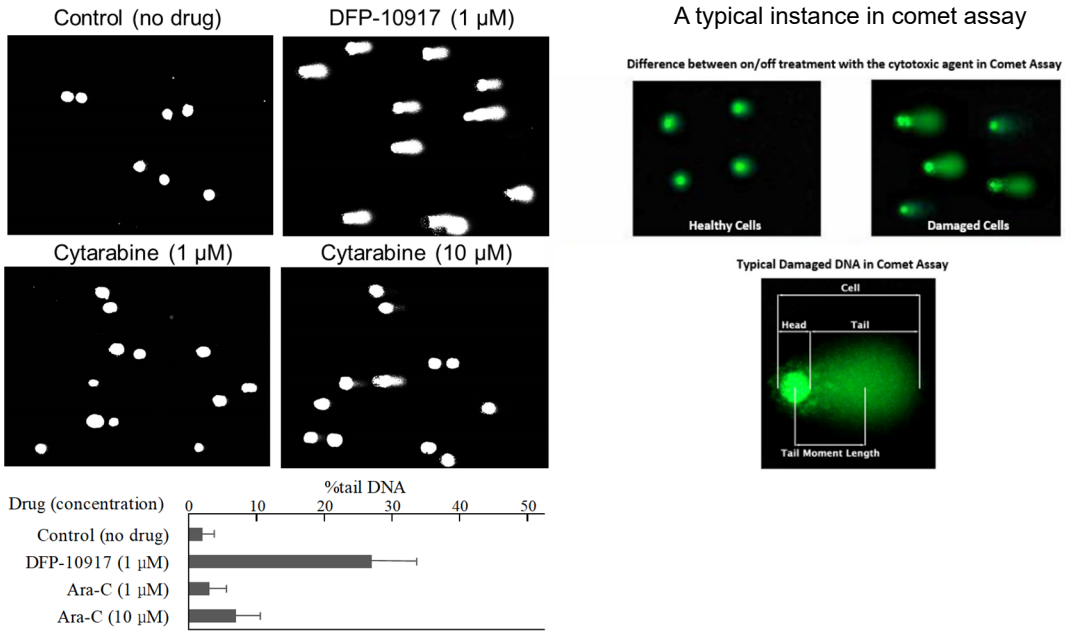

Figure 4.6. DNA fragmentation in CCRF-CEM cells treated with DFP-10917 and cytarabine for 24 h and a typical instance in comet assay.

CCRF-CEM cells ($2x10^5$) were inoculated into 20 ml of culture flask and 24 h later, 1 μM DFP-10917 and 1 to 10 μM cytarabine (IC_{50-70}) were added to the flask, followed by further incubation for 24 h. The cells were then collected and drug-induced DNA fragmentation in the cells was evaluated by the rate of electrophorated DNA (% tail DNA).

Similarly, DNA damage as an indicator of DNA strand breaks by 0.05 µM DFP-10917 and 0.03 µM GEM (both IC_{50} values) was evaluated and calculated as % tail DNA using HeLa cells. The rate of DNA fragmentation (% tail DNA) for 72-h incubation was 7.16±6.86 for the control group, 21.69±12.67 for the DFP-10917 group and 8.37±6.45 for the GEM group (Figure 4.7). These result suggest that DFP-10917 induces potent DNA damage as evaluated by DNA fragmentation (comet assay) compared to cytarabine and GEM.

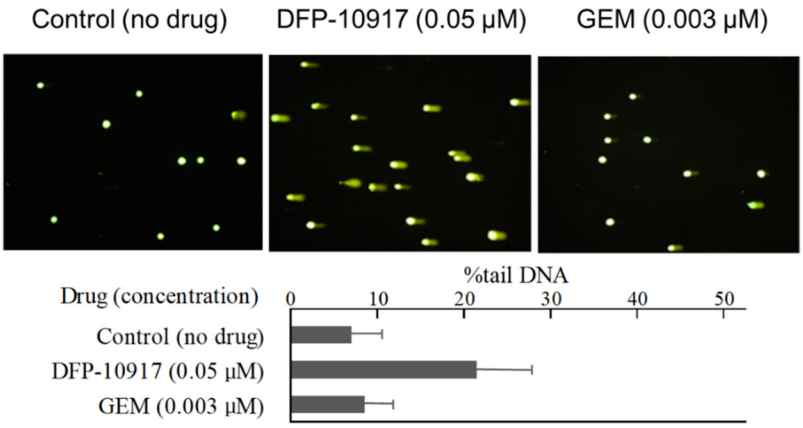

Figure 4.7. DNA damage in HeLa cells treated with 0.05 µM DFP-10917 and 0.003 µM GEM (both IC_{50} values) for 24 h.

HeLa cells ($1x10^6$) were inoculated into 20 ml of culture flask and followed by further incubation for 72 hours. Thereafter, the drug-treated cells were collected and DNA fragmentation induced by the drug was analyzed by comet assay.

4.3.7 Effect of DFP-10917 and GEM on cell-cycle of human tumor cells.

To investigate whether DFP-10917 and GEM, similar cytidine analogs, have similar functions in tumor cells, HeLa cells was exposed for various amounts of time to various concentrations of both drugs, and the numbers of treated cells in the G0/G1, S and G2M of the cell cycle were respectively determined by a cell cycle analyzer. As

shown in Figure 4.8, long-term exposure (72 h) to 1 μM DFP-10917 significantly increased the numbers of cells in the G2/M phase of the cell cycle (G2/M arrest), whereas a high dose (30 μM) and a shorter incubation time (24 h) with this drug resulted in a decrease in the numbers of cells in the S phase, suggesting the inhibition of DNA synthesis under such conditions. By striking contrast, GEM caused only a decrease in the numbers of cells in the S phase when used for 24 h at high (0.3 μM) concentrations. GEM also did not increase the cell number in the G2/M phase of the cell cycle. These results suggest that the functional mechanism of the prolonged exposure to low-dose DFP-10917 clearly differs from that of exposure to GEM or other deoxycytidine analogs.

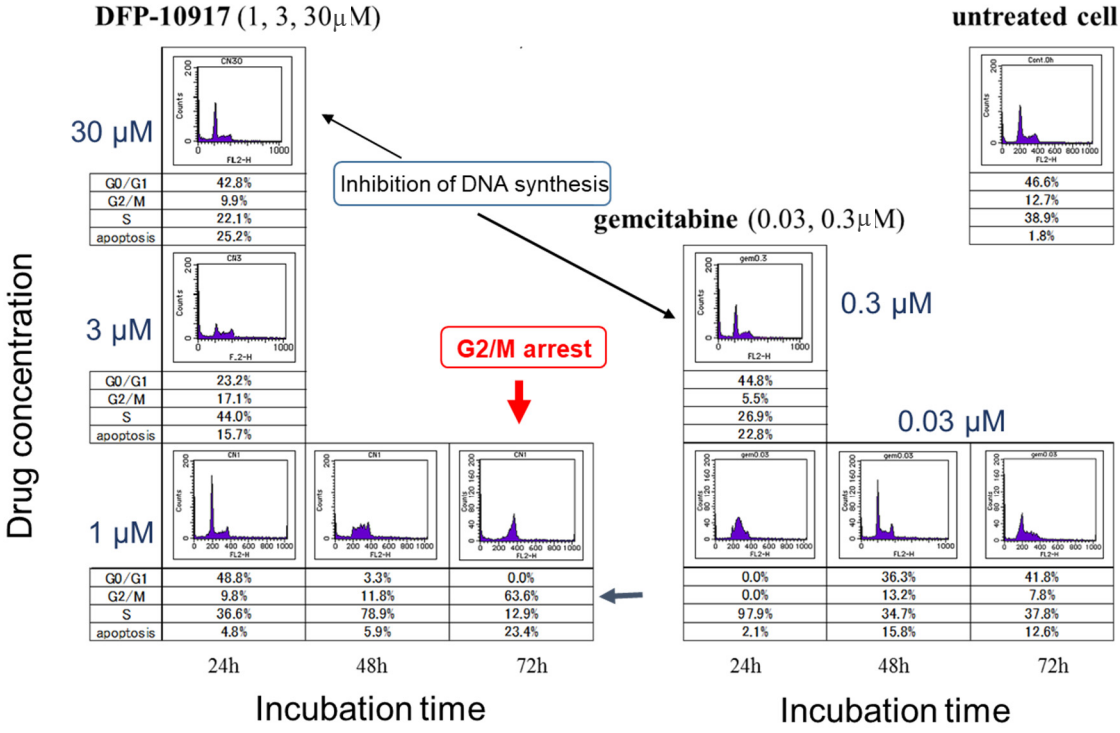

Figure 4.8. Effects of treatment with DFP-10917 and gemcitabine (GEM) on the cell cycle of HeLa cells.

HeLa cells ($1x10^6$) were treated with 1 to 30 μM DFP-10917 and 0.03 to 0.3 μM GEM for 24, 48 and 72 h, and the treated cells were then immediately collected and the distribution rate (%) of cell number in G0/G1, S and G2/M fraction of drug-treated cells was measured using a cell cycle analyzer.

4.4 Discussion

Of the anti-metabolites widely used in the treatment of cancers, antitumor nucleosides, such as cytarabine, GEM and decitabine have been recognized to play a vital role in the treatment of hematological and solid cancers as single agent and/or combined therapeutic regimens. The major mechanisms for the antitumor activity of these cytosine nucleosides is the inhibition of DNA replication or repair, which is much higher in tumor cells than in normal cells via the inhibition of key enzymes, such as DNA polymerases and ribonucleotide reductase or direct incorporation into DNA. However, due to the unfavorable intracellular metabolism (particularly catabolism) of these nucleosides, it would be important to establish suitable exposure conditions, such as dosage and the administration time, in order to reach a desirable antitumor activity with limited toxicity which leads to the objective exhibition of their DNA regulation mentioned above.

DFP-10917 (also kown as CNDAC) is a unique synthesized promising deoxycytidine analog which has been shown to exert potent anticancer activity against various murine and human tumors *in vitro* and *in vivo*[44, 46]. Different from GEM and cytarabine, the cytotoxic mechanism of DFP-10917 has been speculated to be the induction of DNA strand breakage following its incorporation into DNA and the arrest in the G2/M phase of the cell cycle in treated tumor cells[49, 51]. However, the association between the cumulative dosage and treatment schedule of DFP-10917 in order to exert a maximal antitumor activity has not been yet defined *in vivo* human tumor models. In this research, thus the effects of cumulative dose and infusion schedule on the antitumor efficacy of DFP-10917 using KM20C human tumor xenografts in mice was evaluated. As shown in Figure 4.3.A and 4.3.B, when a total of 63 mg/kg of DFP-10917 was administered over a 14-day therapeutic period, the prolonged continuous infusion (14

days) with the lowest dose (4.5 mg/kg/day) resulted in the maximal tumor growth inhibition (tumor regression) with no drug-related toxicity in compared to 1-day infusion with the high doses (30 mg/kg/day, total of 60 mg/kg) or 3-day infusion with the intermediate doses (8 mg/kg/day, total of 48 mg/kg).

Furthermore, the prolonged (14-day) infusion of DFP-10917 was comparatively evaluated in human lung cancer Lu-99 xenografts in which GEM showed limited antitumor activity. As shown in Figure 4.2, the 14-day infusion of low-dose (4.5 mg/kg/day) DFP-10917 reduced tumor volume, while the weekly intravenous injection of high-dose GEM (300 mg/kg) resulted in only a 33% decrease on day 14 and 14% of tumor growth inhibition (TGI) on day 29 in the same therapeutic periods.

The author was interested in investigating whether the prolonged continuous infusion of DFP-10197 at a lower dose also plays the same role in human leukemia cells *in vivo* compared to cytarabine which is a standard therapeutic drug used in the treatment of patients with AML. Thus, the growth inhibitory effect of the 14-day infusion of low-dose DFP-10917 (4.5 mg/kg/day) and consecutive iv injection (days 1-5 and days 8-12) of high-dose cytarabine (100 mg/kg/day) on U937 and MV-4-11 human leukemia tumor xenografts in nude mice was comparatively evaluated, respectively. The prolonged infusion of low-dose DFP-10917 markedly suppressed tumor volume in both leukemia xenografts, and compared to DFP-10917, the repeated 5-day consecutive administration of cytarabine was less effective on these tumors (Figure. 4.5), suggesting that DFP-10917 may be useful for the treatment of leukemia.

In terms of finding the optimal dose of GEM in preclinical and clinical reports, there are various reports over the past 2-3 decades. Veerman *et al*[64] suggested that the prolonged infusion of GEM led to a better antitumor activity than bolus injections *in vivo*

and that it showed promise of being active in clinical trials. On the other hand, Kirstein *et al*[65] showed that long-term survival was significantly diminished following continuous infusion compared with the short-term infusion of GEM, although treatment induced apoptosis following both short-term and continuous infusions in non-small cell lung cancer cells *in vitro*. In clinical trials, Rajdev *et al*[66] performed a phase I trial of GEM administered as a 96-h continuous intravenous infusion in patients with advanced carcinoma and lymphoma and concluded that the administration of GEM as a 96-h infusion resulted in a markedly different toxicity profile than when administered by a conventional 30-min infusion. In addition, a number of clinical studies have supported a short-time (30-min) infusion rather than a long-term (over 2.5 h) infusion of GEM from the viewpoint of the survival and GEM-induced toxicity profiles in cancer patients[67, 68].

Cytarabine, the other deoxycytidine analog, is the standard of care for the treatment of patients with AML. Although there are few reports of the optimization of the dosing schedule of cytarabine in preclinical studies using leukemia cells, various clinical trials have been carried out to determine a suitable or optimal dosing schedules of cytarabine for patients with AML[69-80]. Currently, for the treatment of patients with AML, the 7-day infusion of standard-dose cytarabine (100-200 mg/m^2) or the 6-day infusion of the 12-h high-dose cytarabine (2,000 mg/m^2) in combination with anthracycline (idarubicin or daunorubicin) are conducted as induction therapy, and/or 3-h infusion of high-dose cytarabine (HiDAC, 3,000 mg/m^2) every 12 h/day for 3 to 4 cycles is the consolidation therapy. Accordingly, the dose and schedule of GEM and cytarabine used in this *in vivo* study would reflect the clinical treatment regimen and the prolonged continuous infusion of low-dose DFP-10917 and may contribute to the treatment of patients with solid tumors or leukemia cells resistant or insensitive to standard of

deoxycytidine analogs in future clinical studies.

As regards the molecular and pharmacological mechanisms of DFP-10917 (also known as CNDAC), although Azuma *et al*[49] and Liu *et al*[51] reported that DFP-10917 caused the DNA strand breaks and subsequent G2/M phase arrest of the cell cycle in DFP-10917-treated tumor cells, the strength of DNA damage in solid tumor (HeLa) and leukemia (CCRF-CEM) cells, respectively, induced by low-dose and the prolonged exposure to DFP-10917 compared to treatment with GEM and cytarabine were evaluated. By comet assay, DFP-10917 was confirmed to induce DNA damage by inducing DNA strand breaks (mainly double-strand breaks) in both cells. On the other hand, GEM and cytarabine did not cause such events at the concentrations and exposure times used, which suggests a marked difference in the mechanisms of action between DFP-10917 and the two deoxycytidine analogs, as regards the pharmacological mechanism of the drugs (Figures 4.6 and 4.7). Furthermore, the influence of DFP-10917-induced DNA damage on the cell cycle of HeLa cells *in vitro* and compared the effects to those of GEM was investigated. It was found that only low-dose (1 μM) and long-term exposure (72 h) to DFP-10917 fairly increased the population of cells in the G2/M phase, while 0.003 to 0.03 μM GEM used in this study did not lead to such an accumulation of cells in the G2/M phase of the cell cycle (Figure 4.8). These data are consistent with those of previous studies on several leukemia cells *in vitro*[49-53]. Importantly, these *in vitro* mechanistic experiments were performed based on the finding of which the prolonged infusion of low-dose DFP-10917 attained the regression of tumor growth without any toxicities on human solid and hematological tumor xenografts compared to clinically available deoxycytidine analogs. Accordingly, DFP-10917, when infused consecutively for a long-term period at a low dose, may be a beneficial therapy, not only for hospitalized, but also for outpatients

with advanced and inoperable tumors, including AML and pancreatic cancer. Another clinical phase I/II trial for DFP-10917 administered by continuous infusion has finished in patients with relapsed or refractory AML, which failed to respond to treatment with a cytarabine-containing standard regimen.

In conclusion, based on the cellular metabolism of DFP-10917 and its possible utility strategy, various treatment schedules were investigated using human tumor xenografts in mice and found that the prolonged continuous infusion rather than the short-term administration provided the best outcome for the treatment of the rapid growth of tumor cells *in vivo*. Such an antitumor activity by DFP-10917 was suggested to be depend on the induction of DNA damage and the subsequent accumulation of cells in the G2/M phase (namely G2/M arrest) of the cell cycle in tumor cells *in vitro*, which is markedly different from the functional mechanisms of other antitumor nucleosides.

Chapter 5 Development of Intraperitoneal-delivered RNAi Molecule, DFP-10825

5.1 Introduction

There are a lot of advantages of siRNA drugs for the efficacy in basic research. However, the way to clinical applications of siRNA drugs still have significant barriers in the following example, instability under physiological conditions by ribonuclease, possible immunogenicity, off-target effects and poor cellular uptake[81]. Many different approaches to treatments have been tried in order to solve these barriers, but few practicable treatments have been found so far. With that kind of background, it is necessary to extract the key components of module from the patient information for resolve the issues of siRNA drugs as the strategy for “Module Drug Discovery”.

Peritoneal carcinomatosis (PC), caused by advanced abdominal malignancies, such as those of the ovarian and gastrointestinal (gastric and pancreatic) tracts, has an extremely poor prognosis in the world. Therefore, the development of specific intraperitoneal (ip) drugs using newly emerging cytotoxic and molecular targeted compounds, or new drug delivery systems is an urgent unmet need and essential to improve the efficacy, without severe side-effect, of the ip therapy in patients[82]. In ovarian cancer, the recurrence rate of advanced stage III-IV patients is estimated over 85% and their long-term prognosis is very poor[83, 84]. Therefore, control of recurrent ovarian cancer in the abdominal cavity is thought to be one of the best ways of the increasing survival rate in ovarian cancer. At present, ip chemotherapy with paclitaxel plus cisplatin in addition to intravenous paclitaxel and cisplatin has attained the most prolonged median survival time (MST) in patients with PC[85, 86]. However, the problem with the therapy is substantially toxicity which bone marrow suppression associcted with severe leucopenia

and thrombocytopenia in the ip chemotherapy group, and it is recommended to add a reduction of the toxicity from just ip injection since it could be due to the combination of iv administration. Accordingly, such an ip approach with taxane and platinum drugs has not yet become a routine practice[87]. To improve the outcome in patients with peritoneal disseminated ovarian cancer, new drugs with low toxicity focused on the ip administration are just developing from a viewpoint of inhibition of target molecules in disseminated ovarian cancer[88-91].

Regarding the rapidly-growing ovarian cancer cells, there are several pieces of evidence that thymidylate synthase (TS), an important rate-limiting enzyme in tumoral DNA biosynthesis, has highly expressed in both original and metastatic (peritoneal) ovarian carcinomas[92-95]. The TS expression level (in both protein and gene expression levels) in tumor has been suggested as the key determinant for the efficacy, and the insensitive and resistant of TS-targeting drugs including 5-FU and pemetrexed was innervated by a status of the high and elevated levels of TS expression which target the regulation of post-transcription of *TYMS* expression. Therefore, a monotherapy to control the *TYMS* expression and/or combination with antagonists of TS would be a better approach for the antitumor activity.

In 2011, Kadota *et al* reported that when intratumorally administered, TS-inhibiting vector downregulated the expression of TS mRNA and resultantly overcame the resistance to 5-FU in human colon cancers[96]. Based on this evidence, Abu Lila *et al* tried to develop a liposome-based drug delivery system containing shRNA for TS instead of adeno-virus vector and evaluated the efficacy of PEG-coated shRNA-liposome by intravenous administration in human colorectal cancer cells and also malignant pleural mesothelioma cells *in vitro* and *in vivo*[97, 98].

Because of instability of bare RNAi molecule or its conjugate with liposome in the blood stream following an intravenous injection, and the requirement of rigorous controlling for the particle size of shRNA-liposome (up to 100 nm), a local administration of the shRNA-liposome is rather favorable for locally advanced malignant tumors. Abu Lila showed that the downregulation of TS by RNAi molecules enhanced the antitumor activity of Pemetrexed, the TS inhibitor in an orthotopic mesothelioma model in mice[99].

In this research, DFP-10825 (TS shRN-lipoplex) was developed the assembling deliver and administration system focused on a RNAi effect, which the ip injection of TS shRNA-attached with liposome in peritoneal disseminated human ovarian cancer, based on the supposition that each composition of "Module" are shRNA, intraperitoneal route, cationic liposome, anticancer drug and ovarian cancer in accord with the more common and unmet medical need as the module drug discovery.

5.2 Materials and methods

5.2.1 Materials

Short-hairpin RNA for Thymidylate synthase (TS shRNA, Figure 5.1) for the clinical use by scaling-up synthesis was obtained from Nitto-Denko Avecia Biotechnology Inc. (Massachusetts, USA). Paclitaxel was purchased from Wako Pure Chemical Inc. (Tokyo, Japan). Dioleoylphosphatidylcholine (DOPC) and dioleoyl-phosphatidylethanolamine (DOPE), and O,O'-ditetradecanoyl-N-(α-trimethyl ammonioacetyl) diethanolamine chloride (DC-6-14) for preparation of cationic liposome (called Lipoplex) were provided from NOF Inc. (Tokyo, Japan) and Nippon Fine Chemicals Inc. (Hyogo, Japan), respectively. All other chemicals and biological products used were of the analytical grade commercially available.

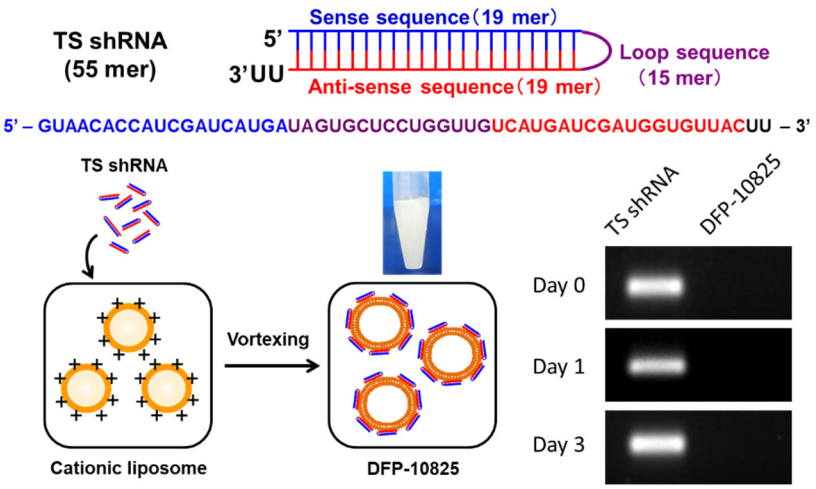

Figure 5.1. New designed structure of RNAi molecule for thymidylate synthase (TS shRNA) and preparation of DFP-10825.

TS shRNA is composed of 19 mer sense sequence, 15 mer loop sequence and 19 mer anti-sense sequence. The preparation of DFP-10825 from TS shRNA, and shRNA-entrapment and -retention of the DFP-10825 after the preparation of cationic liposome (Lipoplexes). As the particle stability for the therapeutic molecules conjugation, the free TS shRNA in the formulation (TS shRNA-lipoplexe, DFP-10825) of 2.0 mg/kg (as shRNA) was checked by agarose gel electrophoresis.

5.2.2 Tumor cells

Human ovarian cancer SKOV3 cells were purchased from DS Pharma Biomedical Co. (Osaka, Japan) and maintained *in vitro* as a monolayer culture in a RPMI-1640 medium-supplemented with heat-inactivated fetal calf serum containing penicillin (100 U/mL), streptomycin (100 μg/mL), and L-glutamine (2 mM). SKOV3 cells expressing firefly luciferase (SKOV3-luc cells) was generated by stable transfection with the firefly luciferase gene (pGL3 basic plasmid; Promega, Madison, WI, USA) in our laboratory and maintained in the same medium until used *in vivo* experiments.

5.2.3 Preparation of cationic liposome (lipoplex)

Cationic liposome composed of DOPE: DOPC: DC-16-4 (3: 2: 5 molar ratio) was prepared by the method of Abu Lila *et al* as described previously[99]. This lipoplex was not constructed a PEG modification.

5.2.4 Preparation of TS shRNA-lipoplex (DFP-10825).

For the preparation of TS shRNA/cationic liposome complex (TS shRNA-lipoplex, DFP-10825, Figure 5.1), TS shRNA and cationic liposome were mixed as a molar ratio of 2,000/1 (lipid:shRNA=2,000:1), and the mixture was vigorously vortexed for 10 min at room temperature to form TS shRNA-lipoplex (DFP-10825). The free TS shRNA in the formulation (TS shRNA-lipoplex, DFP-10825) of 2.0 mg/kg (as shRNA) was checked by agarose gel electrophoresis. As TS-shRNA remained stable in the formulation, no free TS-shRNA was detected up to day 3 after preparation (Figure 5.1). The mean diameter and zeta potential of the DFP-10825 was 395±32 nm and 31±2 mV (n=3), respectively, as determined with a NICOMP 370 HPL submicron particle analyzer (Particle Sizing System, Santa BarbcytarabineA, USA). The concentration of phospholipids was confirmed by colorimetric assay[100]. The absence of free (un-bound) TS shRNA in prepared DFP-10825 was evaluated by electrophoresis performed on 2% agarose gel.

5.2.5 Animals and *in vivo* intraperitoneal orthotopic implantation model

Six- to 8-week-old male SOD/SCID mice were purchased from CLEA Japan IncHFK Animal Technology Co, Ltd. (Beijing, People's Republic of China) and were fed with a sterilized diet and autoclaved water ad libitum. Mice were kept in laminar units

throughout the experiments.

The care and treatment of the animals were in accordance with the guidelines issued by the Science and International Affairs Bureau of the Japanese Ministry of Education, Science, Culture and Sports. The experimental protocol was performed after approval from the Institutional Animal Ethical Committee in Delta-Fly Pharma, Inc (Tokushima, Japan).

Groups of 8-10 SCID mice were used. Intraperitoneally disseminated SKOV3-luc human ovarian cancer models were prepared by ip injection of cultured SKOV3-luc cells (5-10 x 10^6 cells/mouse) into mice, and bioluminescence signals in the tumor-transfected mice were visualized using an *in vivo* imaging system (IVIS, Xenogen, CA, USA). The fluorescence images were acquired using an exposure time of 1/8 second.

5.2.6 Therapeutic efficacy of DFP-10825 in an intraperitoneal disseminated SKOV3-luc cancer model

On day 7 of the peritoneal implantation of SKOV3-luc tumor cells, DFP-10825 (0.5-2 mg/kg as TS shRNA) was administered to the ip cavity in a schedule of ever 3rd day (q3d) for two or four doses. In a combination experiment, Paclitaxel as a dose of 15 mg/kg was intraperitoneally administered to the tumor-bearing mice in the same way above in addition to the DFP-10825 treatment. Tumor bioluminescence imaging (BLI) were checked once a week and body weight twice a week. Antitumor activity of DFP-10825, paclitaxel or their combination was evaluated based on the mean BLI value in the vehicle control and drug-treated groups as follows: Tumor growth inhibition (TGI, %)

= (1 – mean BLI in drug-treated group / mean BLI in control group) x 100.

Survival time of all animals was followed up and the median survival time (MST) was

calculated for each group. Increase in life-span (ILS) was calculated by formula: (MST of treatment group/MST of the control group – 1) x 100 %, and was expressed as the percentage of increase over the life-span of the control animals.

5.2.7 Determination of TS expression levels (TS mRNAs) in SKOV3-luc human ovarian cancer peritoneal disseminated model

TYMS expression (TS mRNA) in ovarian tumor ascites cells and disseminated solid tumors was determined by real-time quantitative RT-PCR of Kadota *et al*[96] and Fujiwara *et al*[101]. Briefly, peritoneal ascetic tumor cells and disseminated tumors were collected from SKOV3-luc-bearing mice and their total RNAs were extracted using RNAiso plus (TAKARA Bio Inc., Shiga, Japan). In this procedure, RNase*Zap* RNase decontamination solution was used throughout to remove possible RNase contamination on benchtop and instruments. First-strand cDNA synthesis was performed with 5-10 μg of total RNA using a cDNA synthesis kit (Amersham Bioscience, Piscataway, NJ, USA). To quantitively measure the *TYMS* expression, TaqMan real-time quantitative PCR was performed with the ABI PRISM 7700 sequence detection system (Applied Biosystems, Foster City, CA, USA). The primers and probes for TS were from Taqman gene expression assay mix (assay ID Hs00426586_m1, lot# 1312626. PCR product size 250 rxns, Thermo Fisher Scientific, Waltham, MA, USA). Each sample was run in triplicates. The comparative threshold cycle method (Applied Biosystems) was used to calculate the gene expression in each sample relative to the value observed in control (no drug) tumor cells, using 18S rRNA (Taqman gene expression assay kit, ID: Hs99999901_s1 18S, size 250 rxns, Thermo Fisher Scientific) as a control for the normalization among samples. RNA samples isolated from 3 mice were evaluated.

5.2.8 Determination of TS shRNA by stem-loop RT-PCR

After ip administration of DFP-10825 (TS shRNA-lipoplex), ascetic fluids and blood samples were isolated from SKOV3-luc-bearing mice, and 100 μL of the 2x denaturing solution and 200 μL of acid phenol-chloroform were added to 100 μL of each isolated sample solution. After vortex for 60 sec and subsequent centrifugation at 10,000 g for 5 min, aliquots (about 100 μL) of aqueous phase were added to 100% ethanol (125 μL), mixed well, moved to filter cartridge, and then centrifuged at 10,000x *g*. The filter cartridge was washed with the mRNA wash solution (700 μL) and then centrifuged. This procedure was repeated three times and subsequently RNA solution from the washed filter cartridge was extracted with nuclease-free water (100 μL) and kept at -80℃ until use in reverse transcription reaction. For TS shRNA, 3 μL of stem-loop RT primer (GTCGTATCCAGTGCAGGGTCCGAGGTATTCGCACTGGATACGACAAAGTAA, HB1404288132, Thermo Fisher Scientific) were added to 5 μL of isolated RNA solution, and incubated at 85℃ for 5 min and at 60℃ for 5 min to denature of RNA. For 18S rRNA as a reference standard, 3 μL of random 9 mers (12.5 μmol/L) were added to the RNA solution (5 μL) and treated by the same way. After that, real-time RT-PCR for TS shRNA and 18S rRNA was performed using TaqMan gene expression kits from Thermo Fisher Scientific, respectively. The TaqMan gene expression kit contains 10 μL Master Mix, 4 μM probe, each 4 μM forward and reverse primer and RT reaction mixture for TS shRNA, and 10 μL Master Mix, small RNA assay for 18S rRNA (20X), nuclease-free water and RT reaction mixture for 18S rRNA. The quantitative PCR was performed with Stratagene MX3005P PCR System (50℃ for 2 min and 95℃ for 10 min in 1 cycle, and then 95℃ for 15 sec and 60℃ for 60 sec in 40 cycles). To analyze the data obtained, the threshold was calculated by MXpro software automatically using the default setting

Export Ct value to Excel. Data of each sample was normalized by using the following formula: ΔCt = Average. Ct (TS shRNA) – Average. Ct (18S rRNA).

Levels of TS shRNA in ascites and blood samples were calculated on the standard curve. By this stem-loop RT-PCR method, TS shRNA was linearly detected at the range of from 15 pM to 228 nM in the ascites and at the range of from 0.6 pM to 228 nM in the blood, respectively, as shown in Figure 5.2.

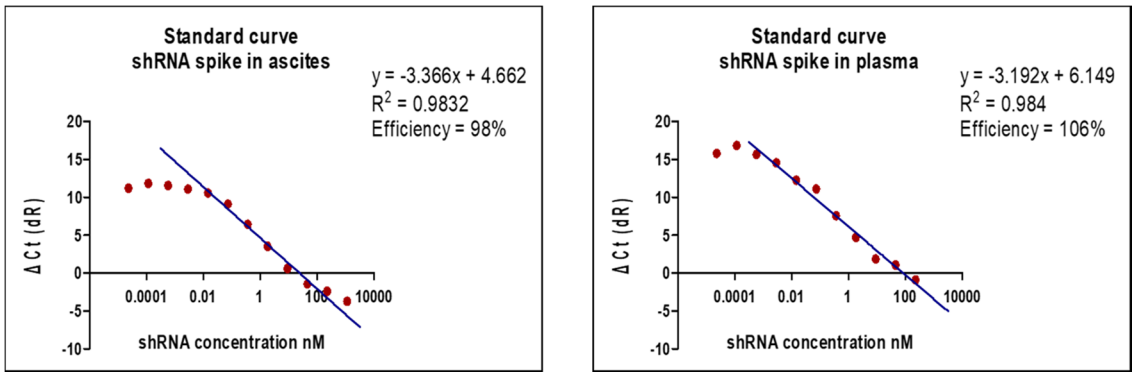

Figure 5.2. Detection range of standard TS shRNA in ascites and plasma in mice bearing intraperitoneally disseminated ovarian cancer cells.

TS shRNA was linearly detected at the range of 15 pM to 228 nM in the ascites and of 0.6 pM to 228 nM in the plasma. ΔCt (dR) was calculated as follows: Δ Ct (dR) = Ct (TS shRNA) – Ct (18S rRNA).

5.2.9 Statistical analysis

The differences between the mean BLI values for comparing groups were analyzed for significance using the one-way analysis of variance (ANOVA). $P<0.05$ was considered statistically significant. The differences between MSTs for comparing groups were analyzed for significance using Wilcoxon test. $P<0.05$ was considered statistically significant.

5.3 Results

5.3.1 Dose dependent tumor growth inhibition by DFP-10825 in peritoneal SKOV3-luc tumor-bearing ascites xenografts in mice

After SKOV3-luc ovarian cancer cells were intraperitoneally inoculated into mice, DFP-10825 of 0.5, 1 and 2 mg as TS shRNA/kg had been intraperitoneally administered for q3d for four dose from 7 days after the inoculation, and the tumor grew to the level monitored the BLI in each group when it reached to ~ 50 photons x 10^7. As presented in Figure 5.3, DFP-10825 at the range of 0.5-1 mg/kg inhibited dose-dependently the growth of ascetic tumor measured as the BLI signal through out of the treatment period from days 7 to 18.

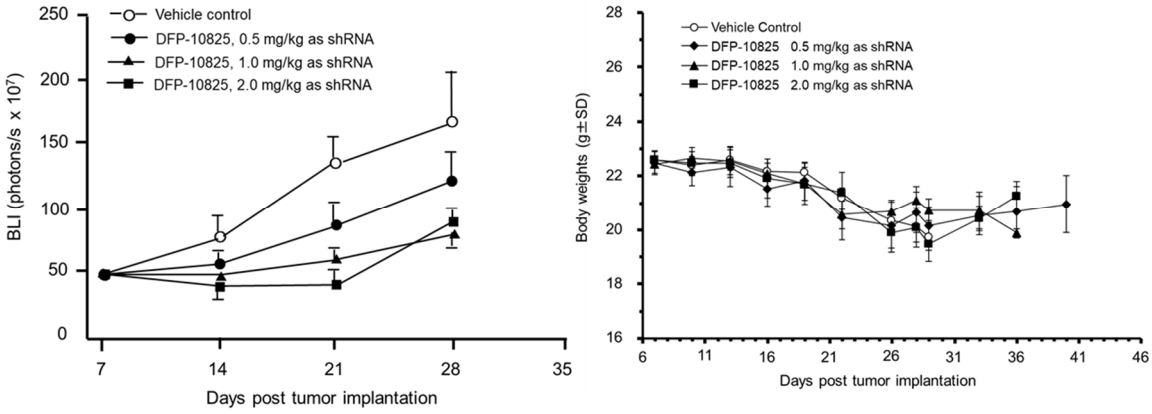

Figure 5.3. Dose dependent antitumor activity and toxicity of DFP-10825 on peritoneal disseminated model of SKOV3-luc human ovarian cancer xenografted into NOD/SCID mice.

BLI: Tumor bioluminescence imaging. After ip inoculation of SKOV3-luc cells (1 x 10^7) into 7 to 8 mice, 0.5, 1 and 2 mg /kg of TS shRNA (with 2,000-fold of lipoplex as molar basis) were intraperitoneally administered, respectively, by schedules of q3d x 4. On day 7, 14, 21 and 28, bioluminescent signals in mouse were monitored and antitumor activity of each dose was evaluated.

The TGI by DFP-10825 at 1 mg/kg reached to plateau, since the next dose (2 mg/kg) and the highest dose tested in the model did not result in further augmented efficacy. The tumor wet weight was measured in the end of the experiment and the consistency between the BLI signals and the tumor wet weight was confirmed (data is not included). To assess the tolerability or toxicity for the ip delivery of DFP-10825, body weight was measured in parallel in this model and no body weight change with DFP-10825 treatment was observed compared to that in the vehicle control group. These data indicate that DFP-10825 as monotherapy against the TS mRNA expression be the effective approach for peritoneal disseminated ovarian cancer without any change in body weight for the host. A typical BLI signal in SKOV3-luc-bearing mice is show in Figure 5.4.

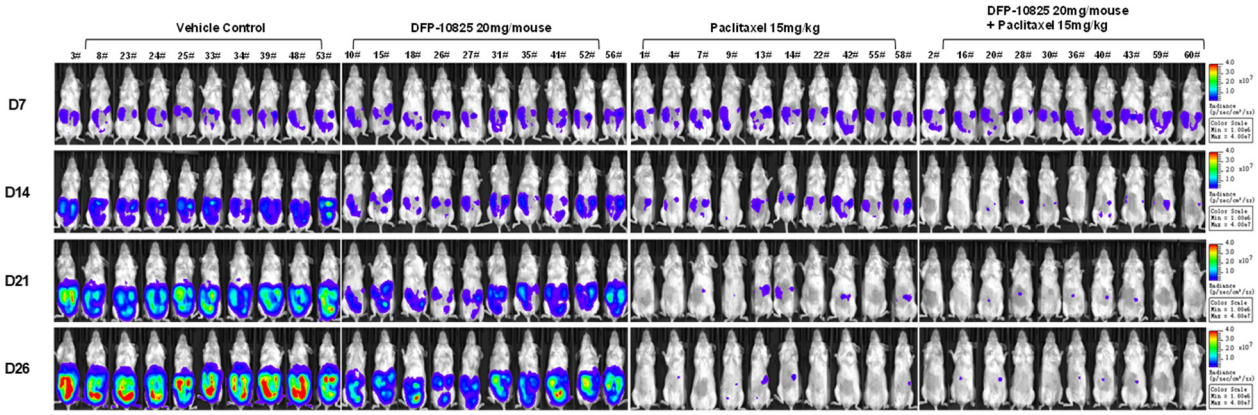

Figure 5.4. Tumor biolumoinescent signals in mice bearing SKOV3-luc tumor cells treated with DFP-10825, paclitaxel and their combination.

After ip inoculation of SKOV3-luc cells (1 x 10^7) into 10 mice, DFP-10825 (1 mg /kg of TS shRNA with 2,000-fold of lipoplex as molar basis), paclitaxel (15 mg/kg) and their combination were intraperitoneally administered, respectively, by schedules of every 3rd day for four doses. On day 7, 14, 21 and 26, bioluminescent signals in each group were monitored.

5.3.2 Antitumor effect of DFP-10825, paclitaxel and their combination on SKOV3-luc tumor ascites model

From Day 7 after SKOV3-luc cells were inoculated into ip cavity of mice, DFP-10825 (1 mg/kg as TS shRNA), paclitaxel (15 mg/kg) and their combination were intraperitoneally administered q3d x 2 times. BLI signals in tumor-bearing mice of each group during the therapeutic periods (days 7 - 28) were illustrated in Figure 5.4. BLI signals in drug-treated mice were found to visually decrease compared with those in the vehicle control group. As shown in Figure 5.5, the treatment with combination of DFP-10825 (as TS shRNA) and paclitaxel was resulted in the significant TGI for the decrease of luciferase-derived BLI signals in mice (in particular, the additive effect was shown better in a log scale). Based on monitored BLI signals in each mouse of each group, antitumor activity (% of TGI) of DFP-10825, paclitaxel and their combination was calculated and presented in Table 5.1. DFP-10825 (1 mg/kg as TS shRNA) resulted in significant (P<0.05) TGI with 56%, 70% and 65% on days 14, 21 and 28, respectively. In this tumor model, ip paclitaxel also showed excellent antitumor activity with TGI of 76%, 96% and 98% on days 14, 21 and 28, respectively. Due to the potent antitumor activity of paclitaxel alone, addition of DFP-10825 to paclitaxel only resulted in a little augmentation of antitumor activity with about 89, 99 and 100% of TGI on days 14, 21 and 28, respectively.

No body weight change in DFP-10825 groups compared to that of the control group was evident. Interestingly, no body weight change in the combination treatment was observed either (Rather slightly increased body weights around 5% over the end of treatment period). Accordingly, in this SKOV3-luc model, it was strongly suggested that DFP-10825, paclitaxel and their combination could be a new therapy option for the

patient with peritoneal disseminated human ovarian cancer and well tolerated for both single and combination therapies.

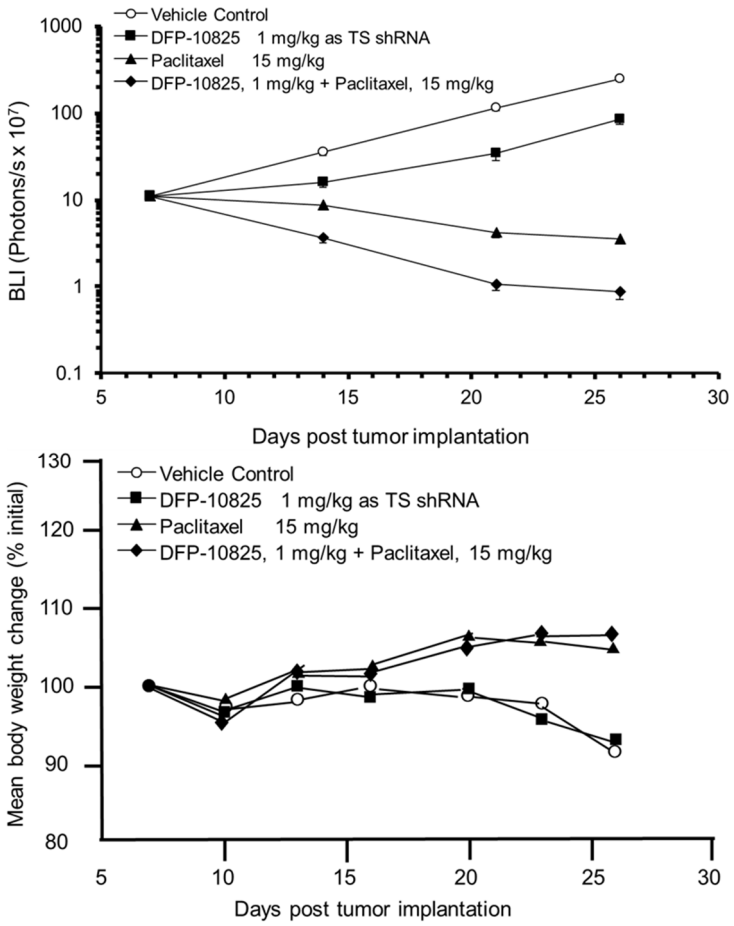

Figure 5.5. Growth inhibitory effect and body weight change of DFP-10825, paclitaxel and their combination on ip disseminated SKOV3-luc tumor xenografts in mice.

From day 7 after *ip* implantation of tumor cells, DFP-10825 (1 mg/kg of TS shRNA with 2,000 fold of lipoplex as molar basis), paclitaxel (15 mg/kg), and their combination were intraperitoneally administered by every 3rd days for two dose, and bioluminescent signals in tumor-bearing mice (n = 10) were monitored on day 7, 14, 21 and 28, respectively. Bioluminescence imaging (BLI) value and tumor growth inhibition (TGI, %) in tumor/bearing mice treated with each drug were shown in detail in Table 5.1.

Table 5.1. Growth inhibitory effects of DFP-10825, paclitaxel and their combination in disseminated ascites model of SKOV3-luc ovarian cancer xenografts.

Group	Day 7	Day 14		Day 21		Day 28	
	(BLI [1])	(BLI [1])	(TGI [2], %)	(BLI [1])	(TGI [2], %)	(BLI [1])	(TGI [2], %)
Vehicle	10.9±0.6	35.3±3.3	-	112.9±8.5	-	240.1±16.6	-
DFP-10825	10.8±0.5	15.5±1.8*	56.1	34.0±6.2*	69.9	84.5±10.8*	64.8
Paclitaxel	10.7±0.5	8.5±1.0**	76.0	4.1±0.5**	96.4	3.5±0.3**	98.5
DFP+Paclitaxel	10.8±0.5	3.7±0.5**	89.5	1.0±0.2**	99.1	0.9±0.2**	99.6

On day 7, 14, 21 and 28 after inoculation of SKOV3-luc cells into mice, tumor growth in each mouse was calculated as BLI signals, and growth inhibitory activity of DFP-10825, paclitaxel and their combination were evaluated as % of TGI to vehicle group. [1] Tumor bioluminescent, [2] Tumor growth inhibition. *, ** significantly different (P<0.05, P<0.01, respectively) from vehicle control group. Data presented as mean ± SD unless otherwise indicated.

5.3.3 Life-prolonging effect in SKOV3-luc-beraing mice by the treatment with DFP-10825, paclitaxel and their combination

After the drug treatments, survival time in mice (n = 10) was monitored for 100 days after the tumor implantation. As shown in Table 5.2, the median survival time (MST) for vehicle control, DFP-10825, paclitaxel and DFP-10825 plus paclitaxel groups was 29, 34, 62 and 83 days, respectively, and increase in life span (ILS) in DFP-10825, paclitaxel and their combination was 17.2% (P=0.007), 113.8% (P<0.01) and 186.2% (P<0.01), respectively. It is worth pointing out that the combination treatment with DFP-10825 and paclitaxel showed an additive effect in parallel with that in the inhibition of tumor growth (Figures 5.4 and 5.5). This further supports the notion that the combination therapy can be a better option as it completely controls the TS activity at both transcriptional and protein levels.

Table 5.2. Survival rates in NOD/SCID mice bearing peritoneal disseminated cells of SKOV3-luc ovarian cancer xenografts treated with DFP-10825, paclitaxel, and their combination.

Treatments	Doses	MST [1] (days)	ILS [2] (%)	P value [3]
Vehicle control	non	29.0	-	-
DFP-10825	1 mg/kg [4]	34.0	17.2	< 0.01
Paclitaxel	15 mg/kg	62.0	113.8	< 0.01[#]
DFP-10825+Paclitaxel	1 mg/kg [4] + 15 mg/kg	83.0	186.2	< 0.01[##]

After drug treatment, survival time in mice (n=10) was respectively monitored throughout 100 days after tumor implantation. MST was 29 days for vehicle control, 34 days for DFP-10825 alone, 62 days for paclitaxel alone, and 83 days for combination of DFP-10825 with paclitaxel. [1] Median survival time, [2] Increase in life span, [3] significantly different from control group for MST, [4] as shRNA dose. [#] Significantly different (P<0.01) from DFP-10825 group. [##] Significantly different (P =<0.01) from paclitaxel group.

5.3.4 TS shRNA levels in ascites and blood for post-intraperitoneal injection of DFP-10825 in SKOV3-luc tumor-bearing ascites mice.

The ip delivered DFP-10825 sufficiently inhibited the growth of intraperitoneally disseminated SKOV3-luc cells in mice and resultantly prolonged the survival of the tumor-bearing mice. To confirm the specificity and PK profile of DFP-10825 (TS shRNA) in peritoneal disseminated this tumor cells, it is important to detect TS shRNA level in the peritoneal ascites and blood stream of mice post injection of DFP-10825. After administration of DFP-10825 (1 mg/kg as TS shRNA), TS shRNA contents in ascites and blood of the tumor-bearing mice (n = 3) were measured at 2, 4, 8 and 24 hours and shown in Figure 5.6. Throughout 24 hours after the administration, the level of TS shRNA could be detected in the ascetic fluids, and TS shRNA concentration in ascites

samples was 4.26±1.00, 3.85±0.78, 1.79±0.51 and 0.68±0.24 nM at 2, 4, 8 and 24 hours post-dosing, respectively. The concentration of ascites at pre-dosing was 2.23±0.54 mL and after 24 hours from the shRNA dosing was 0.61±0.49 mL. By striking contrast, 0.005±0.002 nM of TS shRNA was detected in the bloodstream at 2 hours post-dosing. These results indicate that TS shRNA after the local delivery of DFP-10825 reached a sufficient concentration to control the TS mRNA expression and maintained at a nM range in the ascites up to 8 hours without meaningful detection of the bloodstream. This support the effectiveness and desirable PK profile for the local delivery system of DFP-10825 and further contribute the specific activity via the down-regulation of TS mRNA expression that results in the inhibition of ovarian cancer ascites cells growth while having little adverse events in accordance with the very limited systemic distribution, the desired PK.

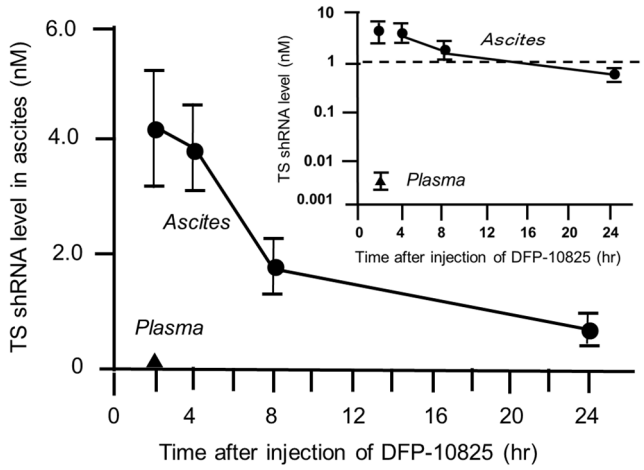

Figure 5.6. TS shRNA levels in ascites fluid and plasma of SKOV3-luc-bearing mice following ip administration of DFP-10825.

TS shRNA levels in ascites were maintained at nM range (0.8-4.5 nM) across 24 hours while those in plasma were extremely low (under 5 pM) at 2 hours after administration of DFP-10825 and half-life time ($T_{1/2}$) of TS shRNA showed 8.8 hours in ascites. Small figure in the upper right was presented as log scale on the y axis.

5.3.5 Inhibition of *TYMS* expression in SKOV3-luc tumor ascites cells after ip administration of DFP-10825.

To demonstrate mode of action of the specificity for the antitumor activity of DFP-10825 in SKOV3-luc tumor ascites cells, the expression of TS mRNA in this tumor cells with ascites was investigated at 24 hours after treatment with DFP-10825. As presented in Figure 5.7, DFP-10825 significantly (P<0.05) downregulated the expression of TS mRNA while paclitaxel did not affect the expression. The suppression of TS mRNA expression (P<0.1) in the combination therapy appears to be due to the action of DFP-10825. Accordingly, it is suggested that the ip administration of DFP-10825 inhibit the growth of disseminated ovarian cancer ascites cells in peritoneal cavity via downregulation of the TS mRNA expression.

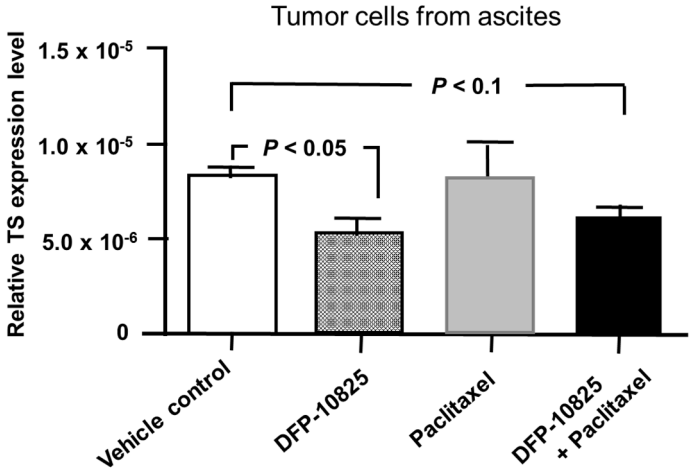

Figure 5.7. TS mRNA expression levels in ip tumor cells of ovarian cancer-bearing ascites mice after ip DFP-10825

18s rRNA was used as the normalization control. Relative gene expression level of TS was $2^{-\Delta Ct}$ [-ΔCt = average Ct (TS) – average Ct (18S rRNA)]. TS mRNA expression was significantly suppressed in ascites tumor cells at 24 hours after ip administration of DFP-10825 alone or in combination with paclitaxel. In this experiment, paclitaxel alone did not down-regulated the expression of TS mRNA in ascites tumor cells.

5.4 Discussion

Ovarian cancer is the most lethal malignancy in the field of gynecology and the peritoneal dissemination is the most frequent type of metastasis of such a type of advanced cancers, which results in a poor prognosis, with 5-year survival of rate <25% [102]. In addition to systemic chemotherapy including taxane and platinum drugs, ip chemotherapy with cytotoxic drugs for the peritoneal carcinomas of ovarian cancer suggested promising clinical effects[103]. Furthermore, a combination of systemic and ip chemotherapy administration of paclitaxel and cisplatin (CDDP) confers a significant survival benefit upon patients with optimally debulked ovarian cancer compared with systemic administration alone[87]. Armstrong *et al*[85] reported that the median survival was prolonged from 49.7 months for systemic paclitaxel + CDDP arm to 65.6 months for a combination of systemic and ip paclitaxel + CDDP regimen. However, there was substantially more toxicity in the combination regimen including severe leucopenia, thrombocytopenia and pain. Accordingly, new agents or novel therapeutic methods focused on disseminated ascetic tumors existing in peritoneal cavity are urgently needed to further improve the survival rate in a better tolerated fashion for the limited therapeutic options to peritoneal disseminated ovarian cancer patients.

The *TYMS*-targeted specific RNAi molecule[96], one of the important rate-limiting enzyme of DNA biosynthesis in rapidly growing tumor cells, was attempted to apply, to treat peritoneal disseminated ascites tumor cells. For this, TS shRNA (Figure 5.1) was conjugated with cationic liposome[88, 89] (named as DFP-10825) and intraperitoneally injected to disseminated SKOV3-luc human ovarian cancer xenograft model in mice. As presented in Figures 5.1 and 5.2, DFP-10825 in the range of 0.5-2 mg/kg as the TS shRNA content and strongly inhibited the growth of SAKOV3-luc ascites cancer cells in the

peritoneal cavity of mice. The same as other malignant cancers such as gastric, colorectal, pancreatic and non-small cell lung cancer, TS expression in ovarian cancer is one of prognostic factors[92-95], and therefore its regulation would lead to improve outcome of a therapy for the ovarian cancer. The result obtained by this data clearly show that regulation of *TYMS* (TS mRNA) by TS shRNA molecule including DFP-10825 not only inhibited the tumor growth but also possibly improved patient's outcome. To further confirm the pharmacokinetic/ pharmacodynamics of such the antitumor activity of DFP-10825 as TS shRNA upon peritoneal disseminated SKOV3-luc ovarian cancer cells, the concentration of TS shRNA in the ascites and blood stream of mice following the ip administration of DFP-10825 on day 28 after inoculation of SKOV3-luc ascites cells was investigated. As shown in Figure 5.6, when 1 mg/kg of TS shRNA was injected, TS shRNA level was found to be sustainable in the range of a single digit nM in the ascites for a long-time (over 24 hours), but not in the bloodstream. This level of TS shRNA is indeed sufficient for its downregulation of *TYMS* expression consistant with the *in vitro* inhibition (IC_{50}, 2.5 nM) of tumor cell viability reported by Abu Lila *et al*[97]. Also a single dose of 1 mg/kg TS shRNA significantly ($P<0.05$) down-regulated the expression of TS mRNA in SKOV3-luc ascites cells in the peritoneal cavity in an *in vivo* system was demonstrated as shown in Figure 5.7.

In the clinical practice, the intraperitoneally dosing paclitaxel in combination with a systemic delivery of chemotherapeutic agents including itself has been frequently used for the treatment of peritoneal disseminated ovarian cancer patients. Therefore, a potential combination opportunity of DFP-10825 with paclitaxel on the anticancer activity and side effects in the same SKOV3-luc tumor model was evaluated. As presented in Figures 5.4 and 5.5, the combination of DFP-10825 with paclitaxel

significantly enhanced the antitumor activity in the disseminated SKOV3-luc tumors compared to that of a single agent of DFP-10825 or paclitaxel. In parallel, the survival rate in the SKOV3-lun tumor-bearing ascites mice was significantly (P<0.01) prolonged to 186 % from 17.2 % for DFP-10825 alone and 113.8 % for paclitaxel alone. However, the host body weight change in the combination was neglectable. Accordingly, the ip administration of DFP-10825 in combination with local delivery of paclitaxel would provide a new ideal therapeutic option for treating the peritoneal disseminated ovarian cancer patients who are sensitive or resistant to paclitaxel.

Recently, several nucleic acid-based drugs have been designed and developed for the treatment of cancers. Those are mainly miRNAs or siRNAs which were coated (or conjugated) with cationic lipid, neutral lipid emulsion and amphoteric liposome[104], and are being extensively investigated in preclinical and clinical stages. For example, Let-7b and miR-34 both suspended in a neutral lipid emulsion, miR-29b attached with liposomes and miR-200c coated with an amphoteric liposome have been intravenously administered and evaluated in non-small cell lung cancer preclinical models and patients with non-small cell lung cancer[105-107]. As a unique therapeutic delivery, miR-16-based mimic miRNA (named as TargomiRs) loaded to targeted bacterial mini cells has been delivered intravenously to cancer patients[108, 109]. Different from RNAi molecules, synthetic antisense-oligonucleotide targeting ribonucleotide reductase R2, a key enzyme in DNA synthesis, has also been investigated pre-clinically[110] and clinically[111, 112] by the method of intravenous infusion for a long-term effect.

In general, nucleic acid-based molecules such as siRNA and miRNA are well known to be unstable in the blood stream due to the rapid hydrolysis by nucleases, and therefore surfactants such as polyethylene glycol are attached to siRNA and miRNA

conjugated with lipids to exhibit their sustained stability in the blood stream. When pegylated DFP-10825 (TS shRNA-cationic liposome) was systemically administered, it sensitized malignant pleural mesothelioma xenografts[94]. However, it is desired to deliver such agents locally to be able to concentrate enough agent as well as avoid any adverse events from systemic delivery system. The peritoneal delivery of DFP-10825 for the peritoneal disseminated ovarian tumor is a good example for such desired therapeutic outcomes with wide therapeutic index, and this success formulation for the delivery system which be maintained with effective concentration for a long period will be paved a new path to further treatment in patients with such the ovarian cancer. In addition, the delivery system can be extended to other PC like peritoneal disseminated human gastrointestinal (gastric and pancreatic) cancers and our preliminary data with the antitumor activity of ip-delivered DFP-10825 in luciferase gene-transfected human gastric and pancreatic cancer xenograft models further confirmed such promising potential (A separate manuscript is being prepared and will be presented in detail later). A clinical trial of the ip DFP-10825 for patients with the peritoneal disseminated ovarian and also other cancers are been planned to undergo in the near future.

Chapter 6 Conclusions

The author proposed "Module Drug Discovery" as a new strategy of drug discovery. This strategy was the creation of new drug by improvement and modification for the existing drugs or the active substances in module units based on the efficacy and safety information for cancer patients. “Module” was defined as a convertible functional unit as pharmaceutical viewpoint. The functional units of “Module” were included chemical compound, small molecular, polymer, antibody and nucleic acid etc., but are not limited to, administration, dose, route, prodrug, drug delivery systems and disease etc. In other words, the creators recognize each element of drugs as functional conversion for modulator by biochemical approach and assemble them to develop new pharmaceutical products as though it was introduced a strategy for general-purpose engineering approach used in manufacturing products or functional units. In this dissertation, the three examples of anticancer drugs were presented as a practical research by using “Module Drug Discovery”.

In the first example, DFP-11207 was made drug discovery by each module which was ascertained the validity of the allegations from the pharmacokinetics and pharmacodynamics profiles and the antitumor activities *in vitro* and *in vivo*. This drug discovery was conducted to compare the difference of the S-1 and DFP-11207 based on conversion from FT to EM-FU as the 5-FU prodrug (one of the module), non-conversion of CDHP as DPD inhibitor (one of the module), and conversion from Oxo to CTA as OPRT inhibitor (one of the module), which the assembling three components focused on the toxicity and antitumor activity of S-1 as one molecule. Following the oral administration, it was confirmed that DFP-11207 was immediately separated to EM-FU,

CDHP and CTA in GI cells, and EM-FU was further converted to the active form of 5-FU by the liver microsomes specifically. On the other hand, released CDHP prevents 5-FU from a rapid degradation (inactivation) in the liver which maintains a persistent plasma 5-FU concentration, and CTA mainly ratained in GI tract cells protected the GI tract from the injury by inhibiting the phosphorylation of 5-FU. In pharmacology study using human tumor xenografts in nude rats, DFP-11207 showed remarkable antitumor activity without any drug-related GI toxicity or thrombocytopenia. The notion of the module drug discovery was strongly supported by creating DFP-11207 as the drug of self-controlled toxicity to the advance of treatment for GI cancer patients.

In the second example, DFP-10917 was practical researched the unique functional mechanism *in vivo* for the active substance, which it caused the DNA double-strand and G2/M cell cycle arrest *in vitro*. It was conducted the comparison with the previous studies and the existing drug focused on the three factors, which they performed the conversion from high dose and short time to low dose and long periods as the administration (one of the module), the adoption of continuous infusion as the route (one of the module), and the selection of hematological cancer as the disease (one of the module). In addition, the association between the dose intensity with the dosing schedule by using the human tumor xenograft models and other analysis methods was aimed to confirm, and the novel functional mechanisms of DFP-10917 compared to other deoxycytidine analogs were elucidated *in vivo*. DFP-10917 was developed the prolonged infusion of low-dose substance mainly displays a novel functional mechanism for the module of the active substance as a DNA-damaging drug. At a range of 0.05 to 1 μM, induced a clear tailed-DNA pattern in both the CCRF-CEM and HeLa cells; cytarabine and GEM did not have any effect. It was thus suggested that a low concentration and long-term exposure to DFP-

10917 aggressively introduced the fragmentation of DNA molecules, namely the so-called double-strand breaks in tumor cells, leading to potent cytotoxicity. Moreover, treatment with DFP-10917 at a low dose with a long-term exposure specifically increased the population of cells in the G2/M phase, while GEM reduced this cell population, suggesting a unique function (G2/M arrest) of DFP-10917. As a result of modifying function of module, DFP-10917 may prove to be useful in the treatment of cancer patients who are resistant to other cytosine nucleosides, or in patients in which these other nucleosides have been shown to be ineffective.

In the third example, DFP-10825 was developed as the therapeutic siRNA drug that was assembled TS-shRNA (as one of the module), intraperitoneal administration (as one of the module), use of cationic liposome and anticancer drugs (as one of the module), and ovarian cancer (as one of the module). DFP-10825 was configured the RNAi molecule for the TS shRNA attached with cationic liposome administered intraperitoneally to the tumor-bearing ascites for the assembling deliver and administration system as a new approach to inhibit the growth of peritoneal disseminated cancer. DFP-10825 showed a dose-dependent antitumor activity in the range of 0.5 to 2 mg/kg as TS shRNA and significantly prolonged the survival rate of the tumor-bearing mice. Furthermore, co-intraperitoneal administration of DFP-10825 and paclitaxel further enhanced the antitumor activity over the efficacy of paclitaxel alone in this tumor model. When intraperitoneally administered, TS shRNA level in ascites but not the blood stream was stably maintained in the range of a single digite nM over several hours and subsequently did down-regulate the expression of TS mRNA in the disseminated SKOV3-luc cell-bearing ascites mice. The results of the assembling modules strongly suggests that the ip delivery of DFP-10825 would provide a new opportunity for improving the outcome of

patients with the peritoneal disseminated ovarian cancer.

These three examples have progressed to the stage of non-clinical or clinical studies at this time[1113, 114], and their takes a little time to be able to use for treatment to the cancer patients in general clinical practice as a proof-of-concept stage. The author is convinced that the strategy of the module drug discovery will be established as a new strategy for drug discovery beyond anticancer drugs.

References

Chapter 1: General Introduction

1. Nwaka S, Ridley RG. Virtual drug discovery and development for neglected diseases through public-private partnerships. Nat Rev Drug Discov. 2003; 2(11): 919-928.
2. Rupp T, Zuckerman D. Quality of Life, Overall Survival, and Costs of Cancer Drugs Approved Based on Surrogate Endpoints. JAMA Intern Med. 2017; 177(2): 276-277.

Chapter 2: Proposal for "Module Drug Discovery" regarding Anticancer Drugs

3. Kneller R. The importance of new companies for drug discovery: origins of a decade of new drugs. Nat Rev Drug Discov. 2010; 9(11): 867-882.
4. Japan Health Sciences Foundation. Medical needs survey for 60 diseases and new medical needs II (Analysis report). Survey report on domestic fundamental technology. 2015 (Japanese).
5. Hanahan D, Weinberg RA. Hallmarks of cancer: the next generation. Cell. 2011; 144(5): 646-674.
6. Collins FS, Varmus H. A new initiative on precision medicine. N Engl J Med. 2015; 372(9): 793-795.
7. National Comprehensive Cancer Network. NCCN Guidelines & Clinical Resources. http://www.nccn.org/professionals/physician_gls/f_guidelines.asp#site.
8. Smith A. Screening for drug discovery: the leading question. Nature. 2002; 418(6896): 453-459.
9. Ashburn TT, Thor KB. Drug repositioning: identifying and developing new uses for existing drugs. Nat Rev Drug Discov. 2004; 3(8): 673-683.
10. Owens PK, Raddad E, Miller JW, Stille JR, Olovich KG, Smith NV, Jones RS,

Scherer JC. A decade of innovation in pharmaceutical R&D: the Chorus model. Nat Rev Drug Discov. 2015; 14(1): 17-28.

11. Zhang B, Fu Y, Huang C, Zheng C, Wu Z, Zhang W, Yang X, Gong F, Li Y, Chen X, Gao S, Chen X, Li Y, Lu A, Wang Y. New strategy for drug discovery by large-scale association analysis of molecular networks of different species. Sci Rep. 2016; 6: 21872.

Chapter 3 Development of New Promising Antimetabolite, DFP-11207

12. Heidelbelger C, Ansfield FJ. Experimental and clinical use of fluorinated pyrimidines in cancer chemotherapy. Cancer Res. 1963; 23: 1226-1243.

13. De Gramont A, Figureer A, Seymour M, Homerin M, Hmissi A, Cassidy J, Boni C, Cortes-Funes H, Cervantes A, Freyer G, Paramichael D, LeBail N, Louvet C, Hendler D, de Braud F, Wilson C, Morvan F, Bonetti A. Leucovorin and fluorouracil with or without oxaliplatin as first-line treatment in advanced colorectal cancer. J Clin Oncol. 2000; 18: 2938-2947.

14. Andre T, Louvet C, Maindrault-Goebel F, Couteau C, Marbro M, Lotz JP, Gilles-Amar V, Krulik M, Carola E, Izael V, de Gramont A. CPT-11 (irinotecan) addition to bimonthly, high-dose leucovorin and bolus and continuous-infusion 5-fluorouracil (FOLFIRI) for pretreated metastatic colorectal cancer, GERCOR. Eur J Cancer. 1999; 35: 1343-1347.

15. Kim NK, Park YS, Heo DS, Suh C, Kim SY, Park KC, Kang YK, Shin DB, Kim HT, Kim HJ. A phase III study of 5-fliorouracil and cisplatin versus 5-fluorouracil, doxorubicin, and mitomycin versus 5-fluorouracil alone in the treatment of advanced gastric cancer. Cancer. 1993; 71: 3813-3818.

16. Caballero GA, Ausman RK, Quebbeman EJ. Long-term, ambulatory, continuous iv infusion of 5-FU for the treatment of advanced adenocarcinomas. Cancer Treat Rep. 1985; 69: 13-15.

17. Quebbeman EJ, Ausman RK, Hansen R, Becker T, Caballero GA, Ritch P, Jenkins D, Blake D, Tangen L, Schulte W. Long-term ambulatory treatment of metastatic colorectal adenocarcinoma by continuous intravenous infusion of 5-fluorouracil. J Surg Oncol. 1985; 30: 60-65.

18. Moynihan T, Hansen R, Anderson T, Quebbeman E, Beatty P, Ausman R, Ritch P, Chitamber C, Vukelich M. Continuous 5-fluorouracil infusion in advanced gastric adenocarcinoma. Am J Clin Oncol. 1988; 11: 461-464.

19. Barbounis VP, Kalofonos HP, Munro AJ, Mckenzie CG, Sackier JM, Epenetos AA. Treatment of colorectal cancer and other malignancies with continuous infusion of 5-fluorouracil. Anticancer Res. 1989; 9: 33-40.

20. Lokich JJ, Ahigren JD, Gullo JJ, Philips JA, Fryer JA. A prospective randomized comparison of continuous infusion fluorouracil with a conventional bolus schedule in colorectal adenocarcinoma: a mid-Atlantic oncology program study. J Clin Oncol. 1989; 7: 425-432.

21. Ishikawa T, Utoh M, Sawada N, Nishida M, Fukase Y, Sekiguchi F, Ishitsuka H. Tumor selective delivery of 5-fluorouracil by capecitabine, a new fluoropyrimidine carbamate, in human cancer xenografts. Biochem Pharmacol. 1998; 55: 1091-1097.

22. Fujii S, Ikenaka K, Fukushima M, Shirasaka T. Effect of uracil and its derivatives on antitumor activity of 5-fluorouracil and 1-(2-tetrahydrofuryl)-5-fluorouracil. Gann. 1978; 69: 763-772.

23. Shirasaka T, Nakano K, Takechi T, Satake H, Uchida J, Fujioka A, Saito H, Okabe

H, Oyama K, Takeda S, Unemi N, Fukushima M. Antitumor activity of 1M tegafur-0.4M 5-chloro-2,4-dihydroxypyridine-1M patasium oxonate (S-1) against human colon carcinoma orthotopically implanted into nude rats. Cancer Res. 1996; 56: 2602-2606.

24. Yen-Revollo JL, Goldberg RM and McLeod HL. Can inhibiting dihydropyrimidine dehydrogenase limit hand-foot syndrome caused by fluoropyrimidines? Clin Cancer Res. 2006; 14: 8-13.
25. Taguchi T. Experience with UFT in Japan. Oncology. 1997; 11 (9 suppl 10): 30-34.
26. Sugimachi K, Maehara Y, Horikoshi N, Shimada Y, Sakata Y, Mitachi Y, Taguchi T. The S-1 Gastrointestinal Cancer Study Group. An early phase II study of oral S-1, a newly developed 5-fluorouracil derivative for advanced and recurrent gastrointestinal cancers. Oncology. 1999; 57: 202-210.
27. Hirata K, Horikoshi N, Aiba K, Okazaki M, Denno R, Sasaki K, Nakano Y, Ishizuka H, Yamada Y, Uno S, Taguchi T, Shirasaka T. Pharmacokinetic study of S-1, a novel oral fluorouracil antitumor drug. Clin Cancer Res. 1999; 5(8): 2000-2005.
28. Shirasaka T, Shimamoto Y, Fukushima M. Inhibition by oxonic acid of gastrointestinal toxicity of 5-fluorouracil without loss of its antitumor activity in rats. Cancer Res. 1993; 53: 4004-4009.
29. Schneider WC. Phosphorus compounds in animal tissues. III. Comparison of methods for the estimation of nucleic acid. J Biol Chem. 1946; 164: 747-751.
30. Fukushima M, Satake H, Uchida J, Shimamoto Y, Kato T, Takechi T, Okabe H, Fujioka A, Nakano K, Ohshimo H, Takeda S, Shirasaka T. Preclinical antitumor efficacy of S-1: a new oral formulation of 5-fluorouracil on human tumor xenografts. Int J Oncol. 1998; 13(4): 693-698.

31. Shirasaka T, Shimamoto Y, Ohshima H, Yamaguchi M, Kato T, Yonekura K, Fukushima M. Development of a novel form of an oral 5-fluorouracil derivative (S-1) directed to the potentiation of the tumor selective cytotoxicity of 5-fluorouracil by two biochemical modulators. Anticancer Drugs. 1996; 7: 548-557.
32. Ikagawa M, Kimura M, Iwai M, Usami E, Yoshimura T, Yasuda K. Neutropenia as a prognostic factor and safety of second-line therapy with S-1 for advanced or recurrent pancreatic cancer. Mol Clin Oncol. 2016; 5: 281-288.
33. Tatsumi K, Fukushima M, Shirasaka T, Fujii S. Inhibitory effects of pyrimidine, barbituric acid and pyridine derivatives on 5-fluorouracil degradation in rat liver extracts. Gann. 1987; 78: 748-755.
34. Ikeda K, Yoshisue K, Matsushima E, Nagayama S, Kobayashi K, Tyson CA, Chiba K, Kawaguchi Y. Bioactivation of tegafur to 5-fluorouracil is catalyzed by cytochrome-450 2A6 in human liver microsomes *in vitro*. Clin Cancer Res. 2000; 6: 4409-4415.
35. Lee JJ, Beumer JH, Chu E. Therapeutic drug monitoring of 5-fluorouracil. Cancer Chemother Pharmacol. 2016; 78: 447-464.

Chapter 4: Development of Novel Deoxycytidine Analog, DFP-10917

36. Noble S and Goa KL. Gemcitabine. A review of its pharmacology and clinical potential in non-small cell lung cancer and pancreatic cancer. Drugs. 1997; 54: 447-472.
37. Barton-Burker M. Gemcitabine: a pharmacologic and clinical overview. Cancer Nurs. 1999; 22: 176-183.
38. Toschi L, Finocchiaro G, Bartolini S, Gioia V and Cappuzzo F. Role of gemcitabine

in Cancer therapy. Future Oncol. 2005; 1: 7-17.

39. Cole N and Gibson BE. High-dose cytosine arabinoside in the treatment of acute myeloid leukemia. Blood Rev. 1997; 11: 39-45.

40. Kern W and Estey EH. High-dose cytosine arabinoside in the treatment of acute myeloid leukemia: Review of three randomized trials. Cancer 2006; 107: 116-124.

41. Reese ND and Schiller GJ. High-dose cytarabine (HD araC) in the treatment of leukemia: a review. Curr Hematol Malig Rep. 2013; 8: 141-148.

42. Li W, Gong X, Sun M, Zhao X, Gong B, Wei H, Mi Y and Wang J. High-dose cytarabine in acute myeloid leukemia treatment: a systematic review and meta-analysis. PLos One. 2014; 9: e110153.

43. Somasekaram A, Jarmuz A, How A, Scott J and Navaratnam N. Intracellular localization of human cytidine deaminase. Identoification of a functional nuclear localization signal. I Biol Chem. 1999; 274: 28405-28412.

44. Azuma A, Nakajima Y, Nishizono N, Minakawa N, Suzuki M, Hanaoka K, Kobayashi T, Tanaka M, Sasaki T and Matsuda A. Nucleosides and Nucleotides. 122. 2'-C-Cyano-2'-deoxy-1-β-D-arabinofuranosylcytosine and its Derivatives. A New Class of Nucleoside with a Broard Antitumor Spectrum. J Med Chem. 1993; 36: 4183-4189.

45. Azuma A, Hanaoka K, Kurihara A, Kobayashi T, Miyauchi S, Kamo N, Tanaka M, Sasaki T and Matsuda A, Nucleosides and Nucleotides. 141. Chemical Stability of a New Antitumor Nucleoside, 2'-C-Cyano-2'-deoxy-1-β-D-arabino-pentofuranosylcytosine in Alkaline Medium: Formation of 2'-C-Cyano-2'deoxy-1-β-D-ribo-pentofuranosylcytosine and its Antitumor Activity. J Med Chem. 1996; 38: 3391-3397.

46. Tanaka M, Matsuda A, Terao T and Sasaki T. Antitumor activity of a novel nucleoside, 2'-C-cyano-2'-deoxy-1-βD-arabinofuranosylcytosine (CNDAC) against murine and human tumors. Cancer Letters. 1992; 64: 67-76.

47. Azuma A, Huang P, Matsuda A and Plunkett W. Cellular pharmacokinetics and pharmacodynamics of the deoxycytidine analog 2'-C-cyano-2'-deoxy-1-β-arabino-pentofuranosylcytosine (CNDAC). Biochem Pharmacol. 2001; 61: 1497-1507.

48. Hayakawa Y, Kawai R, Otsuki K, Kataoka M and Matsuda A, Evidence supporting the activity of 2'-C-cyano-2'-deoxy-1-β-D-arabino-pentafuranosylcytosine as a terminator in enzymatic DNA-chain elongation. Bioorganic & Medicinal chemistry Letters. 1998; 8: 2559-2562.

49. Azuma A, Huang P, Matsuda A and Plunkett W. 2'-C-Cyano-2'-deoxy-1-β-D-arabino-pentofuranosylcytosine: A novel anticancer nucleoside analog that causes both DNA strand breaks and G2 arrest. Mol Pharmacol. 2001; 59: 725-731.

50. Matsuda A, Sasaki T. Antitumor activity of sugar-modified cytosine nucleosides. Cancer Sci. 2004; 95(2): 105-111.

51. Liu X, Guo Y, Li Y, Jiang Y, Chubb S, Azuma A, Huang P, Matsuda A, Hittelman W and Plunkett W. Molecular basis for G2 arrest induced by 2'-C-cyano-2'-deoxy-1-β-D-arabino-pentofuranosylcytosine and consequences of checkpoint abrogation. Cancer Res. 2005; 65: 6874-6881.

52. Wang Y, Liu X, Matsuda A and Plunkett W. Repair of 2'-C-cyano-2'-deoxy-1-β-D-arabino-pantofuranosylcytosine-induced DNA single-starand breaks by transcription-coupled nucleotide excision repair. Cancer Res. 2008; 68: 3881-2889.

53. Liu X, Wang Y, Benaissa S, Matsuda A, Kantarjian H, Estrov Z and Plunkett W. Homologous recombination as a resistance mechanism to replication-induced

double-strand breaks caused by the antileukemia agent CNDAC. Blood. 2010; 116: 1737-1746.

54. Huang P, Chubb S, Hertel LW, Grindey GB and Plunkett W, Action of 2',2'-difluorodeoxycytidine on DNA synthesis. Cancer Res. 1991; 51: 6110-6117.

55. Jiang HY, Hickey RJ, Abdel-Aziz W and Malkas LH. Effects of gemcitabine and ara-C on *in vitro* DNA synthesis mediated by the human breast cell DNA synthesome. Cancer Chemother Pharmacol. 2000; 45: 320-328.

56. Miura S and Izuta S. DNA polymerases as targets of anticancer nucleosides. Curr Drug Targets. 2004; 5: 191-195.

57. Liao W, McNutt MA and Zhu WG. The comet assay: a sensitive method for detecting DNA damage in individual cells. Methods. 2009; 48: 46-53.

58. Food and Drug Administration, HHS. International conference on harmonisation; guidance on S9 nonclincal evaluation for anticancer pharmaceuticals; availability. Fed Regist. 2010; 75: 10487-10488.

59. Cook N, Hansen AR, Siu LL, Abdul Razak AR. Early phase clinical trials to identify optimal dosing and safety. Mol Oncol. 2015; 23: 997-1007.

60. Burris HA 3rd, Moore MJ, Andersen J, Green MR, Rothenberg ML, Modiano MR, Cripps MC, Portenoy RK, Storniolo AM, Tarassoff P, Nelson R, Dorr FA, Stephens CD, Von Hoff DD. Improvements in survival and clinical benefit with gemcitabine as first-line therapy for patients with advanced pancreas cancer: a randomized trial. J Clin Oncol. 1997; 15: 2403-2413.

61. Sandler AB1, Nemunaitis J, Denham C, von Pawel J, Cormier Y, Gatzemeier U, Mattson K, Manegold C, Palmer MC, Gregor A, Nguyen B, Niyikiza C, Einhorn LH. Phase III trial of gemcitabine plus cisplatin versus cisplatin alone in patients

with locally advanced or metastatic non-small-cell lung cancer. J Clin Oncol. 2000; 18: 122-130.

62. Spratlin J1, Sangha R, Glubrecht D, Dabbagh L, Young JD, Dumontet C, Cass C, Lai R, Mackey JR. The absence of human equilibrative nucleoside transporter 1 is associated with reduced survival in patients with gemcitabine-treated pancreas adenocarcinoma. Clin Cancer Res. 2004; 10: 6956-6961.

63. Ho CC1, Kuo SH, Huang PH, Huang HY, Yang CH, Yang PC. Caveolin-1 expression is significantly associated with drug resistance and poor prognosis in advanced non-small cell lung cancer patients treated with gemcitabine-based chemotherapy. Lung Cancer. 2008; 59: 105-110.

64. Veerman G, Ruiz van Haperen VW, Vermorken JB, Noordhuis P, Braakhuis BJ, Pinedo HM and Peters GJ. Antitumor activity of prolonged as compared with bolus administration of 2',2'-difluorodeoxycytidine *in vivo* against murine colon tumors. Cancer Chemother Pharmacol. 1996; 38: 335-342.

65. Kirstein MN, Wieman KM, Williams BW, Fisher JE, Marker PH, Le CT, Yee D and Kratzke RA. Short versus continuous gemcitabine treatment of non-small cell lung cancer in an *in vitro* culture bioreactor system. Lung cancer. 2007; 58: 196-204.

66. Rajdev L, Goldberg G, Hopkins U and Sparano JA. A phase I trial of gemcitabine administration as a 96-h continuous intravenous infusion in patients with advanced carcinoma and lymphoma. Med Oncol. 2006; 23: 369-376.

67. Tempero M, Plunkett W, Ruiz Van Haperen V, Hainsworth J, Hochster H, Lenzi R, Abbruzzese J. Randomized phase II comparison of dose-intense gemcitabine: thirty-minute infusion and fixed dose rate infusion in patients with pancreatic adenocarcinoma. J Clin Oncol. 2003; 21: 3402-3408.

68. Cappuzzo F, Novello S, De Marinis F, Selvaggi G, Scagliotti GV, Barbieri F, Maur M, Papi M, Pasquini E, Bartolini S, Marini L, Crinò L. A randomized phase II trial evaluating standard (50 mg/min) versus low (10 mg/min) infusion duration of gemcitabine as first-line treatment in advanced non-small-cell lung cancer patients who are not eligible for platinum-based chemotherapy. Lung Cancer. 2006; 52: 319-325.

69. Ho DH, Brown NS, Benvenuto J, McCredie KB, Buckels D and Freireich EJ. Pharmacologic studies of continuous infusion of arabinosylcytosine by liquid infusion system. Clin Pharmacol Ther. 1977; 22: 371-374.

70. Kreis W, Chaudhri F, Chan K, Allen S, Budman DR, Schulman P, Weiselberg L, Freeman J, Deere M and Vinciguerra V. Pharmacokinetics of low-dose 1-beta-D-arabinofuranosylcytosine given continuous intravenous infusion over twenty-one days. Cancer Res. 1985; 45: 6498-6501.

71. Spriggs DR, Robbins, Takvorian T and Kufe DW. Continuous infusion of high-dose 1-beta-D-arabinofuranosylcytosine; a phase I and pharmacological study. Cancer Res. 1985; 45: 3932-3936.

72. Donehower RC, Karp JE and Burke PJ. Pharmacology and toxicity of high-dose cytarabine by 72-hour continuous infusion. Cancer Treat Rep. 1986; 70: 1059-1065.

73. Spriggs DR, Sokai JE, Griffin J and Kufe DW. Low dose ara-C administered by continuous subcutaneous infusion: a pharmacologic evaluation. Cancer Drug Deliv. 1986; 3: 211-216.

74. Bolwell BJ, Cassileth PA and Gale RP. Low dose cytosine arabinoside in myelodysplasia and acute myelogenous leukemia: a review. Leukemia. 1987; 1: 575-579.

75. Stentoft J. The toxicity of cytarabine. Drug Saf, 1990; 5: 7-27.

76. Stone RM, Spriggs DR, Dhawan RK, Arthur KA, Mayer RJ and Kufe DW. A phase I study of intermittent continuous infusion high dose cytosine arabinoside for acute leukemia. Leukemia. 1990; 4: 843-847.

77. Schiller G, Gajewski J, Nimer S, Territo M, Ho W, LeeM and Champlin R. A randomized study of intermittent versus conventional-dose cytarabine as intensive induction for acute myelogenous leukemia. Br J Hasematolo. 1992; 81: 170-177.

78. Fleming RA, Capizzi RL, Rosner GL, Oliver LK, Smith SJ, Schffer CA, Silver RT, Peterson BA, Weiss RB, Omura GA, Mayer RJ, Van Echo DA, Bloomfield CD, Schilsky RL. Clinical pharmacology of cytarabine in patients with acute myeloid leukemia: a cancer and leukemia group B study. Cancer Chemother Pharmacol. 1995; 36: 425-430.

79. Bishop JF, Matthews JP, Young GA, Szer SA, Gillett A, Joshua D, Bradstock K, Enno A, Wolf MM, Fox R, Cobcroft R, Herrmann R, Van Der Weyden M, Lowenthai RM, Page F, Carson OM and Juneja S. A randomized study of high-dose cytarabine in induction in acute myeloid leukemia. Blood. 1996; 87: 1710-1717.

80. Lowenberg B, Pabst T, Vellena E, van Putten W, Schouten HC, Graux C, Ferrant A, Sonneveld P, Biemond BJ, Gratwohl A, de Greef GE, Verdonck LF, Schaafsma MR, Gregor M, Theobald M, Schanz U, Maertens J, Ossenkoppele GJ; Dutch-Belgian Cooperative Trial Group for Hemato-Oncology (HOVON) and Swiss Group for Clinical Cancer Research (SAKK) Collaborative Group. Cytarabine dose for acute myeloid leukemia. N Engl J Med. 2011; 364(11): 1027-1036.

81. Xu C, Wang J. Delivery systems for siRNA drug development in cancer therapy. Asian J Pharm Sci. 2015; 10(1): 1-12.

82. Kitayama J. Intraperitoneal chemotherapy against peritoneal carcinomatosis: Current status and future perspective. Surgical Oncology. 2014; 23(2): 99-106.

83. Ozoles RF, Bundy BN, Greer BE, Fowler JM, Clarke-Pearson D, Burger RA, Mannel RS, DeGeest K, Hartenbach EM, Baergen R; Gynecologic Oncology Group. Phase III trial of carboplatin and paclitaxel compared with cisplatin and paclitaxel in patients with optimally resected stage III ovarian cancer: A gynecologic oncology group study. J Clin Oncol. 2003; 21(17): 3194-3200.

84. McGuire WP, Hoskins WJ, Brady MF, Kucera PR, Partridge EE, Look KY, Clarke-Pearson DL, Davidson M. Cyclophosphamide and cisplatin compared with paclitaxel and cisplatin in patients with stage III and stage IV ovarian cancer. New Eng J Med. 1996; 334(1): 1-6.

85. Armstrong CK, Bundy B, Wenzel L, Huang HQ, Baergen R, Lele S, Copeland LJ, Walker JL, Burger RA; Gynecologic Oncology Group. Intraperitoneal cisplatin and paclitaxel in ovarian cancer. New Eng J Med. 2006; 354(1): 34-43.

86. Jaaback K, Johnson N, Lawrie TA. Intraperitoneal chemotherapy for the initial management of primary epithelial ovarian cancer. Cochrane Database Syst Rev. 2011; (11): CD005340.

87. Trimble EL, Alvarez ID. Intraperitoneal chemotherapy and the NCI clinical announcement. Gynecol Oncol. 2006; 103 (2 suppl 1): 518-519.

88. Burger RA, Sill MW, Monk BJ, Greer BE, Sorosky JI. Phase II trial of bevacizumab in persistent or recurrent epithelial ovarian cancer or primary peritoneal cancer: a

Gynecologic Oncology Group Study. J Clin Oncol. 2007; 25(33): 5165-5171.

89. Cannistra SA, Matulonis UA, Penson RT, Hambleton J, Dupont J, Mackey H, Douglas J, Burger RA, Armstrong D, Wenham R, McGuire W. Phase II study of bevacizumain patients with platinum-resistant ovarian cancer or peritoneal serous cancer. J Clin Oncol. 2007; 25(33): 5180-5186.

90. Banerjee S, Kaye SB, Ashworth A. Making the best of PARP inhibitors in ovarian cancer. Nat Rev Clin Oncol. 2010; 7(9): 508-519.

91. Ledermann J, Harter P, Gourley C, Friedlander M, Vergote I, Rustin G, Scott C, Meier W, Shapira-Frommer R, Safra T, Matei D, Macpherson E, Watkins C, Carmichael J, Matulonis U. Olaparib maintenance therapy in platinum relapsed ovarian cancer. New Eng J Med. 2012; 366(15): 1382-1392.

92. Suzuki M, Ohwada M, Tamada T, Tsuru S. Thymidylate synthase activity as a prognostic factor in ovarian cancer. Oncology. 1994; 51(4): 334-338.

93. Look KY, Moore DH, Sutton GP, Prajda N, Abonyi M, Weber G. Increased thymidine kinase and thymidylate synthase activities in human epithelial ovarian carcinoma. Anticancer Res. 1997; 17(4A): 2353-2356.

94. Fujuwaki R, Hata K, Nakayama K, Fukumoto M, Miyazaki K. Thymidylate synthase expression in epithelial ovarian cancer: relationship with thymidine phosphorylase expression and prognosis. Oncology. 2000; 59(2): 152-157.

95. Wang C, Weng Y, Wang H, Shi Y, Ma D. Relationship between the expression of thymidylate synthase, thymidine phosphorylase and dihydropyrimidine dehydrogenase and survival in epithelial ovarian cancer. J Huazhong Sci Technolog Med Sci. 2010; 30(4): 494-499.

96. Kadota K, Huang C-L, Liu D, Yokomise H, Haba R, Wada H. Combined therapy

with a thymidylate synthase-inhibiting vector and S-1 has effective antitumor activity against 5-FU-resistant tumors. Int J Oncol. 2011; 38(2): 355-363.

97. Abu Lila AS, Moriyoshi N, Fukushima M, Huang CL, Wada H, Ishida T. Metronomic S-1 dosing and thymidylate synthase silencing have synergistic antitumor efficacy in a colorectal cancer xenograft model. Cancer Lett. 2017; 400: 223-231.

98. Abu Lila AS, Fukushima M, Huang CL, Wada H, Ishida T. Systemically administered RNAi molecule sensitizes malignant pleural mesotheriomal cells to pemetrexed therapy. Mol Pharm. 2016; 13(11): 3955-3963.

99. Abu Lila AS, Kato C, Fukushima M, Huang CL, Wada H, Ishida T. Downregulation of thymidylate synthase by RNAi molecules enhances the antitumor effect of pemetrexed in an orthotopic malignant mesothelioma xenograft mouse model. Int J Oncol. 2016; 48(4): 1399-1407.

100. Bartlett GR. Colorimetric assay methods for free and phosphorylated glyceric acids. J Biolo Chem. 1959; 234(3): 469-471.

101. Fujiwara H, Terashima M, Irinoda T, Takagane A, Abe K, Kashiwaba M, Oyama K, Takahashi M, Maesawa C, Saito K, Takechi T, Fukushima M. Quantitative Measurement of thymidylate synthase and dihydropyrimidine dehydrogenase mRNA level in gastric cancer by real-time RT-PCR. Jpn J Cancer Res. 2002; 93(12): 1342-1350.

102. Ozols RF. Treatment goals in ovarian cancer. Int J Gynecol Cancer. 2005; 15(suppl 1): 3-11.

103. Markman M. Intraperitoneal antineoplastic agents for tumors principally confined to the peritoneal cavity. Cancer Treat Rev. 1986; 13(4): 219-242.

104. Fortunato O, Boeri M, Verri C, Moro M, Sozzi G. Therapeutic use of microRNAs in lung cancer. Biomed Res Int. 2014; 2014:756975.

105. Trang P, Wiggins JF, Daige CL, Cho C, Omotola M, Brown D, Weidhaas JB, Bader AG, Slack FJ. Systemic delivery of tumor suppressor microRNA mimics using a neutral lipid emulsion inhibits lung tumors in mice. Mol Ther. 2011; 19(6): 1116-1122.

106. Wu Y, Craford M, Mao Y, Lee RJ, Davis IC, Elton TS, Lee LJ, Nana-Sinkam SP. Therapeutic delivery of microRNA-29b by cationic lipoplexes for lung cancer. Mol Ther Nucleic Acids. 2013; 2: e84.

107. Cortez MA, Valdecanas D, Zhang X, Zhan Y, Bhardwaj V, Calin GA, Komaki R, Giri DK, Quini CC, Wolfe T, Peltier HJ, Bader AG, Heymach JV, Meyn RE, Welsh JW. Therapeutic delivery of miR-200c enhances rediosensitivity in lung cancer. Mol Ther. 2014; 22(8): 1494-1503.

108. Reid G, Kao SC, Pavlakis N, Brahmbhatt H, MacDiarmid J, Clarke S, Boyer M, van Zandwijk N. Clinical development of TargomiRs, a miRNA mimic-based treatment for patients with recurrent thoracic cancer. Epigenomics. 2016; 8(8): 1079-1085.

109. Van Zandwijk. Safety and activity of microRNA-loaded minicells in patients with recurrent malignant pleural mesothelioma: a first-in-man, phase 1, open-label, dose-escalation study. The Lancet Oncol. 2017; 18(10): 1386-1396.

110. Lee Y, Vassilakos A, Feng N, Lam V, Xie H, Wang M, Jin H, Xiong K, Liu C, Wright J, Young A. GTI-2040, an antisense agent targeting the small subunit component (R2) of human ribonucletide reductase, shows potent antitumor activity against a variety of tumors. Cancer Res. 2003; 63(11): 2802-2811.

111. Klisovic RB, Blum W, Wei X, Liu S, Liu Z, Xie Z, Vukosavljevic T, Kefauver C, Huynh L, Pang J, Zwiebel JA, Devine S, Byrd JC, Grever MR, Chan K, Marcucci G. Phase I study of GTI-2040, an antisense to ribonucleotide reductase, in combination with high-dose cytarabine in patients with acute myeloid leukemia. Clin Cancer Res. 2008; 14(12): 3889-3895.

112. Sridhar SS, Canil CM, Chi KN, Hotte SJ, Ernst S, Wang L, Chen EX, Juhasz A, Yen Y, Murray P, Zwiebel JA, Moore MJ. A phase II study of the antisense oligonucleotide GTI-2040 plus docetaxel and prednisone as first-line treatment in castration-resistant prostate cancer. Cancer Chemother Pharmacol. 2011; 67(4): 927-933.

Chapter 6: Conclusions

113. https://www.clinicaltrials.gov/ct2/show/NCT02171221?term=DFP-11207&rank=1

114. https://www.clinicaltrials.gov/ct2/show/NCT01702155?term=DFP-10917&rank=1

Acknowledgements

The author would like to express the gratitude to Dr. Tatsuhiro Ishida, Professor of Tokushima University, for his kind guidance and hearty encouragement.

The author greatly appreciate the all adequate guidance and constructive support from Dr. Masakazu Fukushima, Delta-Fly Pharma, Inc.

The author really appreciate the opportunity Dr. Kiyoshi Eshima, Delta-Fly Pharma, Inc. have given me to research the drug discovery.

The author thank Dr. Hiromi Wada and Dr. Chen-Long Huang, Kyoto University, for their helpful suggestion of the clinical application.

The author thank Dr. Chun Zhang, Dr. Cheng Jin, Dr. Mei Hong and Dr. Kokoro Eshima for their assistant in the research preparation and the data management.

Finally, the author grateful to my wife and child for various supports.

List of Publications

This research was published in the following academic journals.

1. Development of new promising antimetabolite, DFP-11207 with self-controlled toxicity in rodents.

   Masakazu Fukushima, **Kenzo Iizuka**, Cheng Jin, Chun Zhang, Mei Hong and Kiyoshi Eshima.

   Drug Design, Development and Therapy. 2017; 11: 1693-1705.

2. Analysis of the prolonged infusion of DFP-10917, a deoxycytidine analog, as a therapeutic strategy for the treatment of human tumor xenografts *in vivo*.

   Kenzo Iizuka, Chun Zhang, Kokoro Eshima, Cheng Jin, Kiyoshi Eshima and Masakazu Fukushima.

   International Journal of Oncology. 2018; 52: 851-860.

3. Anticancer activity of the intraperitoneal-delivered DFP-10825, the cationic liposome-conjugated RNAi molecule targeting thymidylate synthase, on peritoneal disseminated ovarian cancer xenograft model.

   Kenzo Iizuka, Cheng Jin, Kokoro Eshima, Mei Hua Hong, Kiyoshi Eshima and Masakazu Fukushima.

   Drug Design, Development and Therapy. 2018; 12: 673-683.